The Association
of
Engineering and Shipbuilding Draughtsmen.

Axial and Centrifugal Compressor Design for Aircraft Engines.

By NORMAN C. BREDDY.

Published by The Association of Engineering and Shipbuilding Draughtsmen,
Onslow Hall, Little Green, Richmond, Surrey.

SESSION 1956-57.

Price 3/-

Printed by Milne, Tannahill & Methven, Ltd. (T.U.), 12-14 Mill Street, Perth.

ADVICE TO INTENDING AUTHORS OF A.E.S.D. PRINTED PAMPHLETS.

Pamphlets submitted to the National Technical Sub-Committee for consideration with a view to publication in this series should not exceed 10,000 to 15,000 words and about 20 illustrations. The aim should be the presentation of the subject clearly and concisely, avoiding digressions and redundance. Manuscripts are to be written in the third person. Copies of an article entitled "Hints on the Writing of Technical Articles" can be obtained from the Editor of *The Draughtsman*.

Drawings for illustrations should be done either on a good plain white paper or tracing cloth, deep black Indian ink being used. For ordinary purposes they should be made about one-and-a-half times the intended finished size, and it should be arranged that wherever possible these shall not be greater than a single full page of the pamphlet, as folded pages are objectionable, although, upon occasion, unavoidable. Where drawings are made larger, involving a greater reduction, the lines should be made slightly heavier and the printing rather larger than normal, as the greater reduction tends to make the lines appear faint and the printing excessively small in the reproduction. In the case of charts or curves set out on squared paper, either all the squares should be inked in, or the chart or curve should be retraced and the requisite squares inked in. Figures should be as self-evident as possible. Data should be presented in graphical form. Extensive tabular matter, if unavoidable, should be made into appendices.

Authors of pamphlets are requested to adhere to the standard symbols of the British Standards Institution, where lists of such standard symbols have been issued, as in the case of the electrical and other industries, and also to the *British Standard Engineering Symbols and Abbreviations*, No. 1191, published by the B.S.I. at 5/-. Attention might also be given to mathematical notation, where alternative methods exist, to ensure the minimum trouble in setting up by the printer.

The value of the pamphlet will be enhanced by stating where further information on the subject can be obtained. This should be given in the form of footnotes or a bibliography, including the name and initials of the author, title, publisher, and year of publication. When periodicals are referred to, volume and page also should be given. References should be checked carefully.

Manuscripts, in the first instance, should be submitted to the Editor, *The Draughtsman*, Onslow Hall, Little Green, Richmond, Surrey.

For pamphlets, a grant of £20 will be made to the author, but special consideration will be given in the case of much larger pamphlets which may involve more than the usual amount of preparation.

The Publishers accept no responsibility for the formulae or opinions expressed in their Technical Publications.

The Association
of
Engineering and Shipbuilding
Draughtsmen.

Axial and Centrifugal Compressor Design for Aircraft Engines.

By NORMAN C. BREDDY.

Published by The Association of Engineering and Shipbuilding Draughtsmen,
Onslow Hall, Little Green, Richmond, Surrey.

SESSION 1956-57

9/56

AXIAL COMPRESSOR DESIGN FOR AIRCRAFT ENGINES.

By Norman C. Breddy.

The axial flow compressor is based on the conversion of kinetic energy to pressure energy through the medium of rows of moving blades and stator blades which are designed on an aerodynamic basis. As such, the axial compressor provides a smoother gas flow than the centrifugal type and greater pressure ratios are obtainable. From the standpoint of energy transfer the compressor is simply a reversed turbine but there the similarity ends.

The principle of the axial flow compressor is by no means a new invention. C. A. Parsons filed a patent in 1884 which described the use of his reaction turbine as a compressor ; however, it is only during recent years that the difference between an accelerating flow and a decelerating flow has been fully understood.

In all flow phenomena there exists an associated boundary layer in contact with the containing walls, which, because of friction, flows at a decreased velocity. There is a natural tendency for the gas to break away from the walls in a diffusing passage and cause turbulence, or in extreme circumstances result in a backflow. Unless the decelerating process is carefully controlled by aerodynamic theories the boundary layer can become so thick, that the main flow is contained within a channel of constant cross section illustrated in Fig. 1. In such a case P_2 would be only

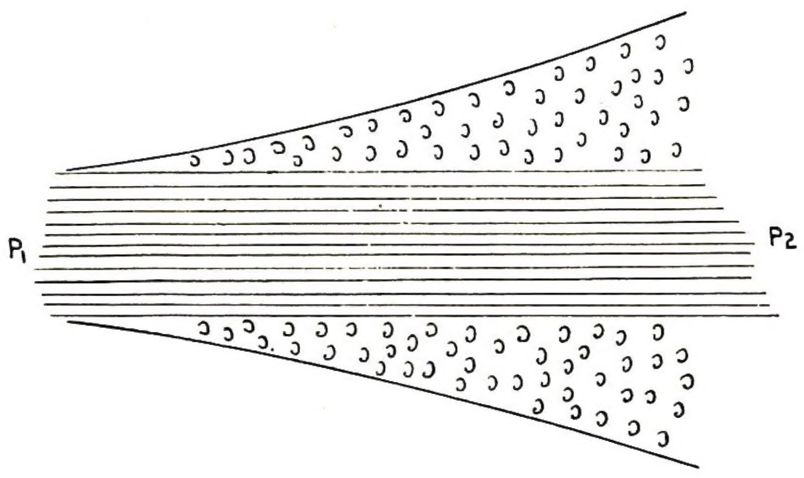

Fig. 1—Inefficient Diffusion Process.

slightly greater than P_1 and therefore practically no velocity change has occurred. During recent years a tremendous amount of data has been obtained by the study of flow past a series of aerofoils known as a cascade, which represents the flow problem of a compressor with a greater degree of accuracy than by using a single aerofoil.

Nomenclature.

U	=	Tangential velocity of blades in feet per sec.
V_a	=	Axial velocity of air through the compressor in feet per second.
V_1	=	Relative velocity of air in feet per sec.
α	=	Air angle.
V_w	=	Whirl components of the absolute air velocities in ft./sec.
W	=	Work done in ft. lbs.
Ω	=	Work done factor.
$\triangle T_{st}$	=	Stage total head temperature rise.
R_{st}	=	Stage total head pressure ratio.
T_{1t}	=	Inlet total head temperature.
η_{st}	=	Total head isentropic efficiency.
$\triangle T_a$	=	Static temperature rise in rotor.
$\triangle T_b$	=	Static temperature rise in stator.
Λ	=	Degree of reaction.
T	=	Static temperature.
A	=	Area in sq. ft.
ϱ	=	Density of air in lb./cu. ft.
L	=	Lift in lbs.
D	=	Drag in lbs.
C_{LP}	=	Lift co-efficient.
C_{DP}	=	Drag co-efficient.
P_{1t}	=	Inlet total head pressure (lbs. per sq. in.)
P_{2t}	=	Outlet total head pressure (lbs. per sq. in.)
P_1	=	Inlet static pressure (lbs. per sq. in.)
P_2	=	Outlet static pressure (lbs. per sq. in.)
$\triangle P$	=	Static pressure rise (lbs. per sq. in.)
F	=	Axial force in lbs.
Q	=	Mass flow in lb. per sec.
y	=	Ratio of specific heats $\frac{Cp}{Cv}$
$T2_t{}^1$	=	Outlet total head temp. for isentropic compression.

General Aerofoil Theory.

Fig. 2 (*a*) represents an aerofoil supported in a wind tunnel in a fixed position with reference to the air stream; *i.e.*, the flow is parallel to the aerofoil. In this case the air is divided around

the section, separating at the leading edge and joining again at the trailing edge. With a well-designed aerofoil there exists no turbulence and the flow is streamlined.

Now let the aerofoil be set at an angle *i* degrees, which is termed the angle of incidence, to the air flow, as shown at Fig. 2 (*b*). In this case a greater disturbance is set up and the flow will be changed although at a point well behind the trailing edge the airstream will resume its normal flow. These local deflections can only occur when the blade exerts a force on the air, thus by Newton's law an equal and opposite reaction takes place on the blade through the

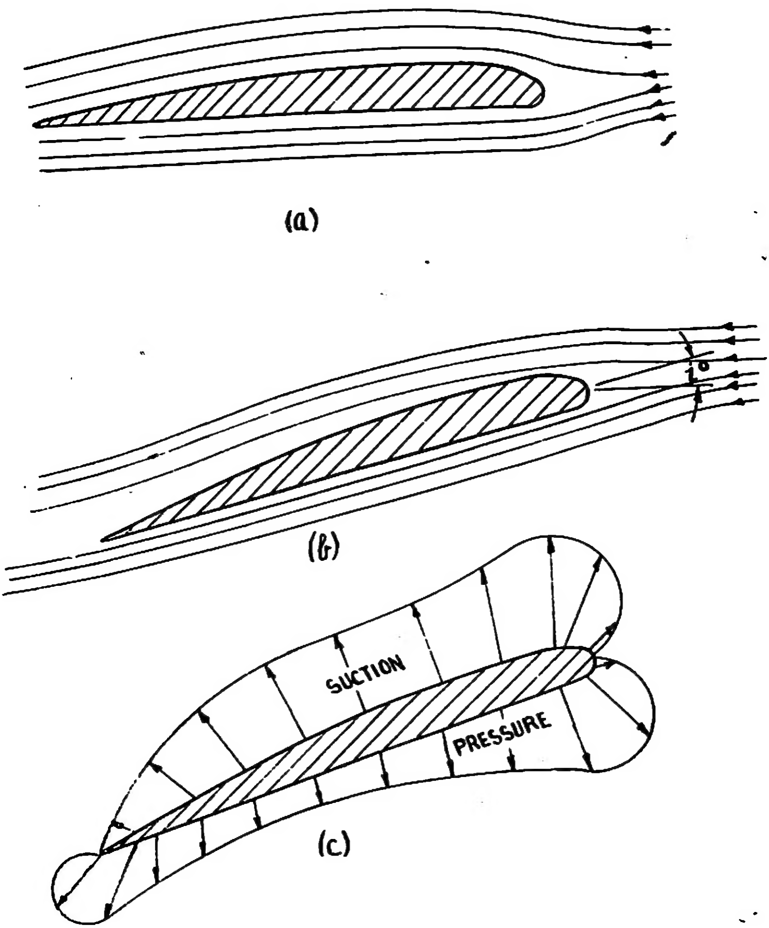

Fig. 2—Air Flow Past an Aerofoil.

medium of the air. Such forces can only appear in the shape of pressure exerted by the air stream on the blade.

By the Bernoulli equation it follows that with local pressure changes along the blade profile there exists velocity changes. Examination of the streamlines over the top of the aerofoil shows that they tend to converge upon each other, thus indicating an increase in velocity, with a corresponding drop in pressure. On the lower side of the aerofoil the streamlines separate indicating a reduced velocity with an increase in pressure. The pressure distribution around such an aerofoil is shown in Fig. 2 (*c*).

The vectorial sum of these pressures will result in a resultant force which can be resolved into L, a lift component and D, a drag component. It is possible to measure the lift and drag force for all values of aerofoil sections, airflow and incidence angle, etc., Fig. 3.

$$\text{Now lift L} = \frac{1}{2g} \varrho \, . \, V^2 \, . \, C_L \, . \, A \qquad (1)$$

$$\text{Drag D} = \frac{1}{2g} \varrho \, . \, V^2 \, . \, C_D \, . \, A \qquad (2)$$

From (1) and (2) has been evolved two co-efficients C_L and C_D relating velocity, area, density and lift or drag forces. Curves can be plotted from wind tunnel tests which can then be employed in calculations relating to the particular aerofoil. The aerodynamics of flow throughout a compressor can be analysed in two ways; (1) as an isolated aerofoil, and (2) as a cascade of aerofoils. The second method is now the accepted one and Fig. 4 illustrates the cascade nomenclature for compressor blading.

Nomenclature.

β_1 = Blade inlet angle.
β_2 = Blade outlet angle.
θ = Blade camber angle = $\beta_1 - \beta_2$.
ζ = Stagger angle.
S = Pitch.
C = Chord.
a = Distance of point of max. camber from the leading edge.
α_1 = Air inlet angle.
α_2 = Air outlet angle.
V_1 = Air inlet velocity.
V_2 = Air outlet velocity.
i = Incidence angle = $\alpha_1 - \beta_1$.
δ = Deviation angle = $\alpha_2 - \beta_2$.
ϵ = Deflection = $\alpha_1 - \alpha_2$.

Lift and Drag Co-efficients of a Cascade of Blades.

In practice it is usual to relate the lift and drag of the cascade to the vector mean (V_m) of the inlet and outlet gas velocities. The axial velocity is assumed to be constant throughout the stage and under such circumstances the velocity diagram of the cascade is shown in Fig. 5.

The static pressure rise across the blades is given by :—

$$\triangle P = P_2 - P_1 = (P_{2t} - \tfrac{1}{2}\varrho V_2^2) - (P_{1t} - \tfrac{1}{2}\varrho V_1^2)$$

$$\therefore \quad \triangle P = \tfrac{1}{2}\varrho (V_1^2 - V_2^2) - \overline{\omega} = \tfrac{1}{2}\varrho Va^2 (\tan^2\alpha_1 - \tan^2\alpha_2) - \overline{\omega} \quad (3)$$

Due to the fact that the density change is negligible the incompressible flow formula is adopted.

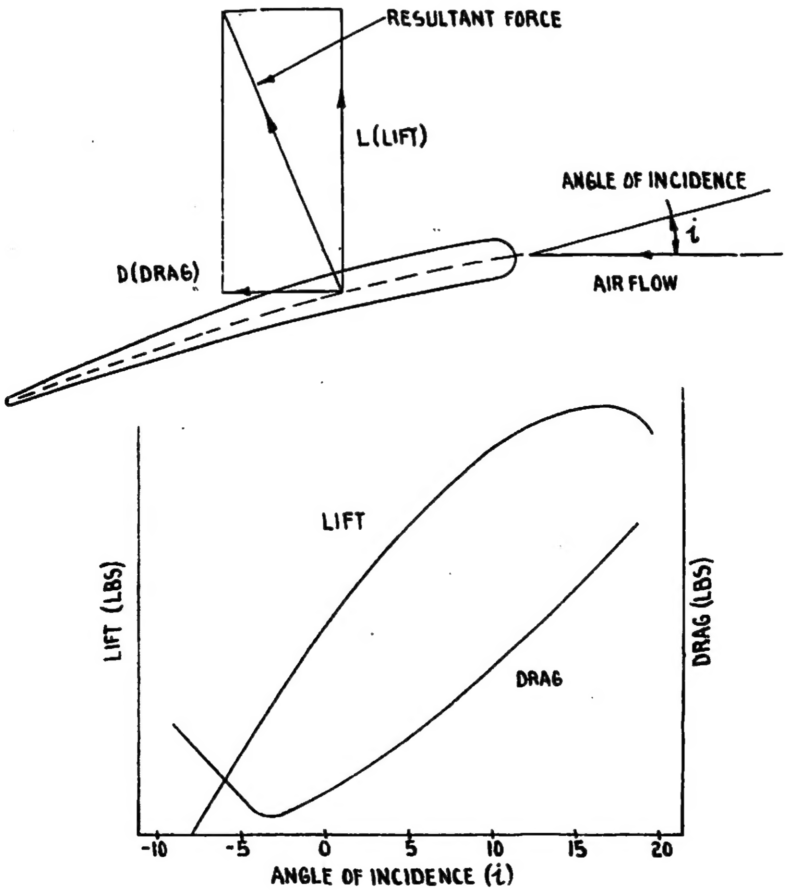

Fig. 3—Forces Acting on an Aerofoil.

The axial force $F = S \cdot \varrho \cdot V_a \times$ change in velocity component along the cascade $= S \cdot \varrho \cdot V_a^2 \ (\tan\alpha_1 - \tan\alpha_2)$ (4)

Now $V_m = V_a \sec \alpha_m$ (5)

and $\tan \alpha_m = \frac{1}{2} (\tan\alpha_1 + \tan\alpha_2)$ (6)

D and L being the drag and lift forces along and perpendicular to the vector mean velocity

$D = \frac{1}{2} \varrho V_m^2 \cdot C \cdot C_{DP} = F \sin \alpha_m - S \cdot \Delta P \cdot \cos \alpha_m$ (7)

From equations (3) and (4) we get :—

$$\tfrac{1}{2} \varrho \cdot V_m^2 \cdot C \cdot C_{DP} = S \cdot \varrho \cdot Va^2 (\tan \alpha_1 - \tan \alpha_2) \sin\alpha_m - S.\tfrac{1}{2}\varrho.V_a^2 (\tan^2\alpha_1 - \tan^2\alpha_2) \cos \alpha_m + S \cdot \cos \alpha_m \cdot \overline{\omega}$$

and since $(\tan^2\alpha_1 - \tan^2\alpha_2) = (\tan \alpha_1 - \tan \alpha_2)(\tan\alpha_1 + \tan\alpha_2)$
$= 2 (\tan \alpha_1 - \tan \alpha_2) \tan \alpha_m$

$$C_{DP} = \frac{S}{C} \cdot \frac{\overline{\omega}}{\frac{1}{2}\varrho} \cdot \frac{\cos \alpha_m}{V_m^2} = \frac{S}{C} \cdot \frac{\overline{\omega}}{\frac{1}{2}\varrho} \cdot \frac{\cos^3\alpha_m}{V_a^2}$$

$$= \frac{S}{C} \cdot \frac{\omega}{\frac{1}{2} \varrho V_1^2} \cdot \frac{\cos^3\alpha_m}{\cos^2\alpha_1} \quad (8)$$

By resolving forces perpendicular to the vector mean V_m

$L = \frac{1}{2} \varrho \cdot V_m^2 \cdot C \cdot C_L = F \cos \alpha_m + S \cdot \Delta P \sin \alpha_m$

Therefore $\frac{1}{2} \varrho V_m^2 \cdot C \cdot C_L = S \cdot \varrho \cdot V_a^2 (\tan \alpha_1 - \tan \alpha_2) \cos \alpha_m - \overline{\omega}\ S \cdot \sin \alpha_m$

$$\therefore C_L = 2 \cdot \frac{S}{C} (\tan \alpha_1 - \tan \alpha_2) \cos \alpha_m - C_{DP} \cdot \tan \alpha_m \quad (9)$$

The term $C_{DP} \tan \alpha_m$ in equation (9) is so small that it can be neglected hence :—

$$C_L = 2 \cdot \frac{S}{C} (\tan \alpha_1 - \tan \alpha_2) \cos \alpha_m \quad (10)$$

Cascade Performance.

Tests are now made on a cascade of blades of known shape at a given stagger angle with a range of incidence and flow velocities. Measurements are taken of the inlet and outlet velocities (V_1 & V_2) along with the air angles (α_1 and α_2) and the pressure difference across the blade row ($P_2 - P_1$). From this data the following quantities can be calculated :—

α_m (Equation (6)).
V_m (Equation (5)).
$\epsilon = \alpha_1 - \alpha_2$.
$i = \alpha_1 - \beta_1$.
$\delta = \alpha_2 - \beta_2$.
ΔP (Equation (3)) and pressure loss co-efficient $\Delta P/\frac{1}{2g}.\varrho.V_1^2$.
C_{DP} (Equation (8)).
C_L (Equation (10)).

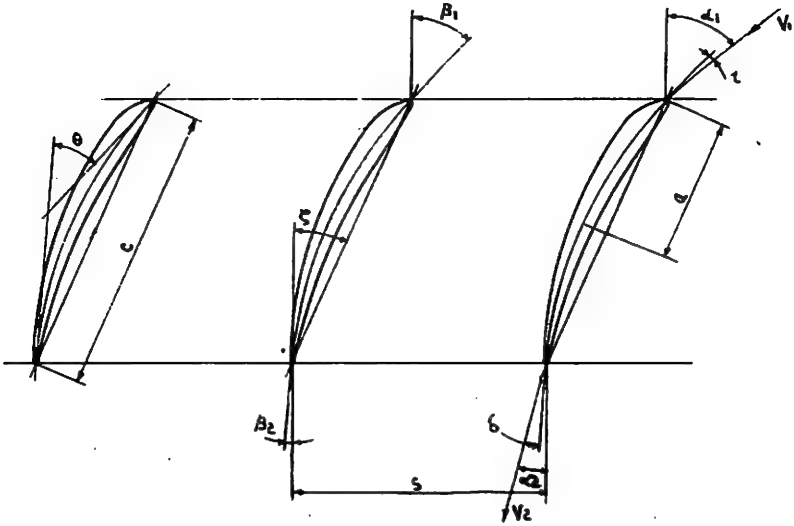

Fig. 4—Cascade Notation.

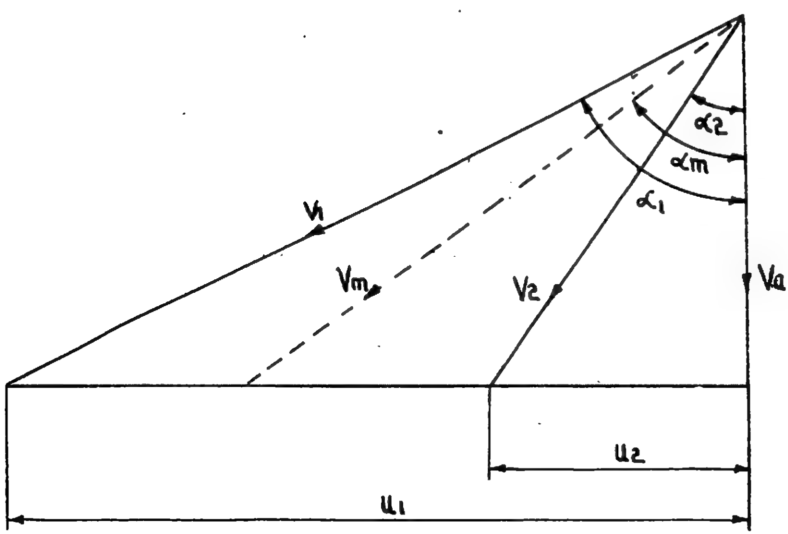

Fig. 5—Velocity Diagram (Constant Axial Velocity).

Fig. 6 illustrates the performance of a compressor cascade. It will be seen that a value of deflection can be selected which is the most suitable for the cascade being considered. The ultimate object of the cascade is to turn the air through the largest angle possible, with a minimum loss, hence the selected deflection will be near the maximum point of the curve.

In order to obtain a high efficiency the ratio $\dfrac{C_L}{C_{DP}}$ should be at a maximum and in this particular example it is about 50. At this figure the deflection is 80% of the maximum deflection. Successive tests carried out on other cascades show similar characteristics; thus it has become a standard practice to adopt a "design point" on a cascade where the deflection is 80% of the maximum obtainable. Design conditions are usually denoted by a star,

$$i.e.,\ \epsilon^* = 0{\cdot}8\ (\alpha_1 - \alpha_2)\ \text{max.} \tag{11}$$

For blades of the same pitch/chord ratio and camber, equal values of ϵ^* are obtained when the corresponding outlet angles α_2 are also equal. Although ϵ^* at any given α_2 decreases as the pitch S increases, the variation with the camber angle θ is only very small and over the range 20-40 degrees, can be disregarded. Therefore design deflection ϵ^* is a function of S/C and α_2. See Fig. 6.

The air outlet angle α_2 for a given blade outlet angle β_2 is measured by the deviation δ which can be estimated from a number of empirical equations. Constants Rule is widely used :—

$$\delta = m\,\theta\ \left(\frac{S}{C}\right)^{\frac{1}{2}} \tag{12}$$

For blades of circular or parabolic camber

$$m = 0{\cdot}23\ \left(\frac{2a}{C}\right)^2 + 0{\cdot}1\ \left(\frac{\alpha_2}{50}\right) \tag{13}$$

When a circular arc camber line is used (13) becomes :—

$$m = 0{\cdot}23 + 0{\cdot}1\ \left(\frac{\alpha_2}{50}\right) \tag{14}$$

Work Done Per Stage.

Fig. 7 represents one stage in an axial flow compressor. Air approaches the rotor blades with an absolute velocity V_0 and at an angle α_0 in combination with a peripheral velocity U. The relative velocity will be V_1 at an angle α_1 as shown by the velocity triangle. The air then passes through the diverging passages which increases its absolute velocity to V_2 at an angle α_2. Due to diffusion $V_2 < V_1$ and thus a pressure rise would have occurred in the rotor. The peripheral velocity U in combination with V_2,

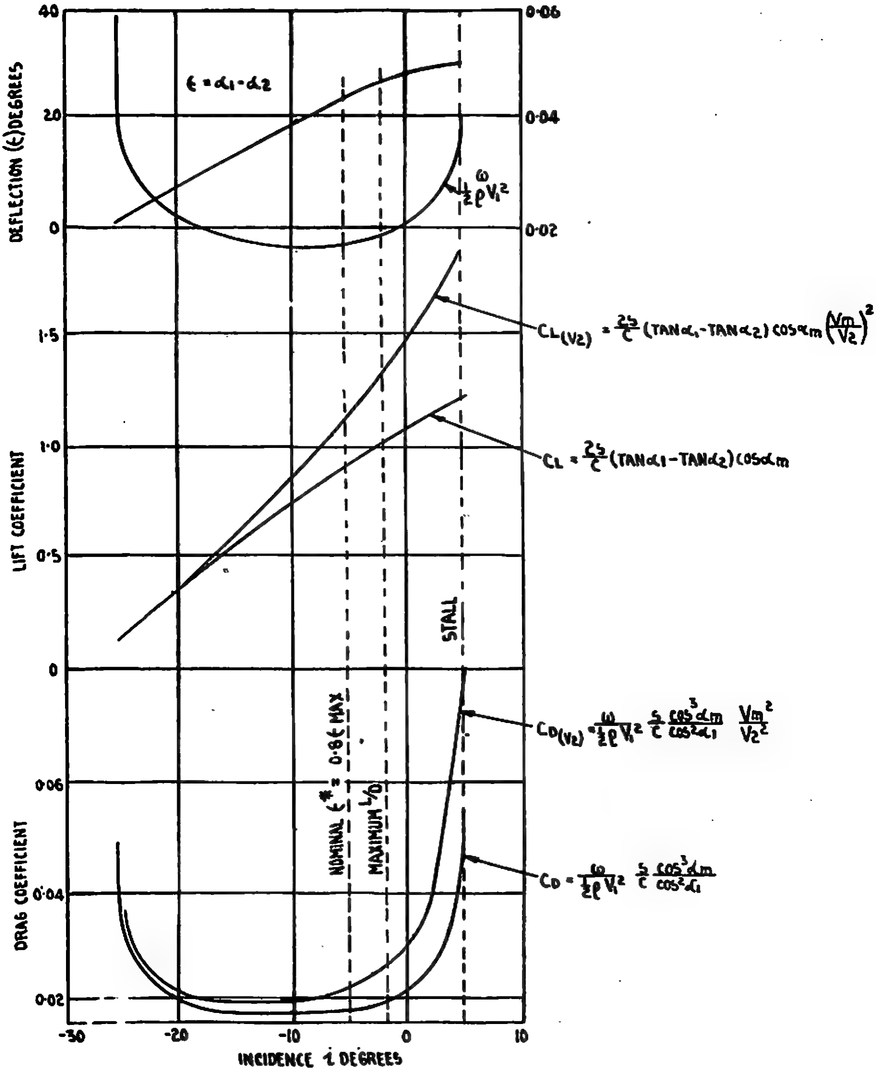

Fig. 6—Performance of a Compressor Cascade.

For $\theta = 33°$, A/C = 0·4, S/C = 0·94, $\beta_2 = 14°$ (from A. R. Howell).

gives the absolute velocity V_3 and outlet angle α_3 at exit from the rotor.

From the geometry of the velocity triangles two basic equations are obtained :—

$$\frac{U}{V_a} = \tan \alpha_0 + \tan \alpha_1 \tag{15}$$

$$\frac{U}{V_a} = \tan \alpha_2 + \tan \alpha_3 \tag{16}$$

The work done on the air in the rotor blades per lb. of air per second is equal to the change in whirl momentum times the distance moved per second.

$$W = \frac{U}{g} \,.\, V_a \,.\, (\tan \alpha_3 - \tan \alpha_0) = \frac{U}{g} \,.\, V_a \,.\, (\tan \alpha_1 - \tan \alpha_2) \tag{17}$$

The energy imparted to the gas will increase the total head temperature a theoretical amount.

$$\Delta T_s = \frac{UV_a}{g \,.\, J \,.\, C_p} (\tan \alpha_1 - \tan \alpha_2) \tag{18}$$

For $J = 1400$ ft. lb. per C.H.U. and $C_p = 0{\cdot}24$ equation (18) reduces to

$$\Delta T_s = 0{\cdot}923 \left(\frac{U}{100}\right) \left(\frac{V_a}{100}\right) (\tan \alpha_1 - \tan \alpha_2) \tag{19}$$

The actual stage temperature rise will be somewhat less than this, due to the fact that the axial velocity V_a is not constant along the blades. The increase in total head temperature is only about 85% to 90% of equation (19) thus :—

$$\Delta T_{st} = \Omega \,.\, 0{\cdot}923 \left(\frac{U}{100}\right) \left(\frac{Va}{100}\right) (\tan \alpha_1 - \tan \alpha_2) \tag{20}$$

where Ω = work done factor.

The stage total-head pressure ratio $Rst = \left(1 + \frac{\eta st \,.\, \Delta Tst}{T_1 t}\right)^{\frac{y}{y-1}}$ (21)

where $T_1 t$ = inlet total head temperature.

η_{st} = total head isentropic efficiency.

Degree of Reaction.

Reaction is the ratio static temperature rise in the rotor to that in the whole stage. Under isentropic conditions this is equal to

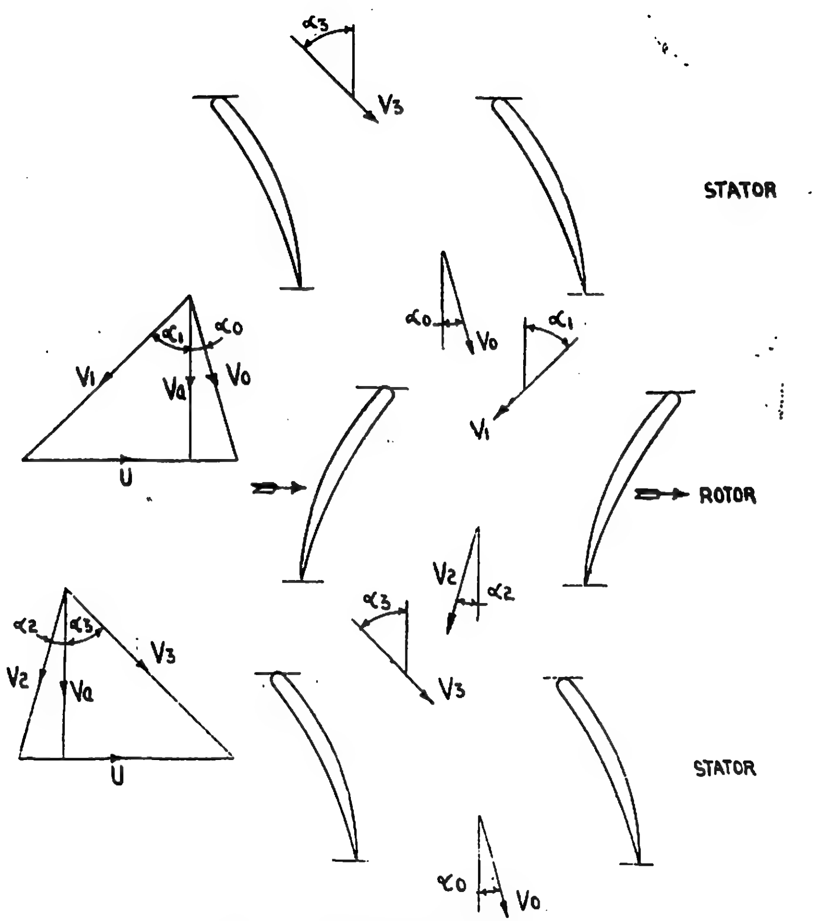

Fig. 7—Axial Compressor Stage.

the corresponding ratio of static pressure rises. The choice of the degree of reaction in compressor design is an important one and an expression can be evolved for a certain degree of reaction in terms of velocities and air angles. The simplest case is one where it is assumed that $V4 = V_o$, *i.e.*, the gas leaves the stage with the same velocity at which it enters it, hence $\Delta Ts = \Delta Tst$.

Putting ΔT_A = temperature rise in rotor.

ΔT_B = temperature rise in stator.

$$\text{Then } W = C_p . J\ (\Delta T_A + \Delta T_B) = C_p . J . \Delta T_s$$

$$= \frac{U . Va}{g} (\tan \alpha_1 - \tan \alpha_2) \tag{22}$$

$$= \frac{U . Va}{g} (\tan \alpha_3 - \tan \alpha_0).$$

$Vo = Va \sec \alpha_0$

$$\therefore\ Vo^2 - V_3^2 = Va^2 (\tan^2\alpha_0 - \tan^2\alpha_3) \tag{23}$$

$V_3 = Va \sec \alpha_3$

$$\text{By substitution } T_2 - T_1 = \frac{UVa}{g . J . Cp} (\tan \alpha_3 - \tan \alpha_0)$$

$$\left\{ 1 - \frac{Va}{2U} (\tan \alpha_3 - \tan \alpha_0) \right\} \tag{24}$$

$$\text{The degree of reaction } \wedge,\ i.e.,\ \frac{\Delta T_A}{\Delta T_s} = \frac{\Delta T_A}{\Delta T_A + \Delta T_B}$$

$$= \frac{U . Va (\tan \alpha_3 - \tan \alpha_0) - \frac{1}{2}Va^2 (\tan^2\alpha_3 - \tan^2\alpha_0)}{U . Va\ (\tan \alpha_3 - \tan \alpha_0)}$$

$$= 1 - \tfrac{1}{2} . \frac{Va}{U} (\tan \alpha_3 + \tan \alpha_0)$$

$$= 1 - \tfrac{1}{2}\ \frac{\tan \alpha_3 + \tan \alpha_0}{\tan \alpha_1 + \tan \alpha_0} \tag{25}$$

In the case of 50% reaction blading where the inlet and exit air angles of the stator are equal to the inlet and exit angles of the rotor.

$$\alpha_1 = \alpha_3 \text{ and } \alpha_0 = \alpha_2 \quad \therefore \text{ from (25) } \wedge = 1 - \tfrac{1}{2}$$

Vortex Flow.

Consideration has so far only been given to the velocity triangles at one particular radius. The peripheral speed U varies proportionately to the radius and the variation of the other velocity vectors will depend on the design. The velocity of air at any point during

the flow through the compressor will possess a component in the peripheral as well as the axial direction, therefore the flow will be a spiral in the direction of rotation, otherwise known as vortex in form. Vortex theory is based on the fact that radial pressure forces act on the air elements in order to obtain the necessary centripetal acceleration in association with the whirl velocity. That is, the whirl velocity varies inversely as the radius which in equation form :—

$$V_w = \frac{\text{constant}}{r}$$

Stage Performance and Pressure Rise.

In addition to the drag co-efficient already mentioned, two additional factors must be taken into account. They are secondary losses, attributed to additional drag in the compressor annulus, tip clearance and trailing vortices. Tip clearance has a big influence on such losses, thus should be kept as small as possible, usually in the region of 1% to 2% of the total blade height. The additional drag co-efficient arising from secondary losses has been approximated by the following empirical formula :—

$$C_{DS} = 0{\cdot}018\, C_L^2 \qquad (26)$$

C_L being the lift Co-efficient given in equation (10).

The annulus drag loss has also been quoted as an empirical formula :—

$$C_{DA} = 0{\cdot}020\, s/h \qquad (27)$$

where s = pitch.

h = height of blades.

$\therefore \quad C_D = C_{DP} + C_{DS} + C_{DA}$

Equation (8) was derived for the straight cascade and will apply equally as well for the annular case. Substituting C_D for C_{DP}

$$C_D = \frac{S}{C} \cdot \frac{\overline{\omega}}{\frac{1}{2}\varrho \cdot V_1^2} \cdot \frac{\cos^3 \alpha_m}{\cos^2 \alpha_1} \qquad (28)$$

$\therefore$ The overall pressure loss for the stage $\dfrac{\overline{\omega}}{\frac{1}{2}\varrho \cdot V_1^2}$

$$= \frac{C_D}{\dfrac{S}{C} \cdot \dfrac{\cos^3 \alpha_m}{\cos^2 \alpha_1}} \qquad (29)$$

If the compression in the blade row takes place according to the polytropic law $\dfrac{P}{\varrho^n} = C$

the efficiency of the process is

$$\eta = \frac{T_{2t}^1 - T_{1t}}{T_{2t} - T_{1t}} = \frac{\left(\frac{P_{2t}}{P_{1t}}\right)^{\frac{y-1}{y}} - 1}{\left(\frac{P_{2t}}{P_{1t}}\right)^{\frac{n-1}{n}} - 1} \tag{30}$$

Putting the loss $\overline{\omega}$ equal to zero and substituting in equation (3) the theoretical pressure rise

$$\triangle P^1 = \tfrac{1}{2}\,\varrho\,.\,V_a^2\,(\tan^2\alpha_1 - \tan^2\alpha_2) = \tfrac{1}{2}\,\varrho\,.\,V_a^2\,(\sec^2\alpha_1 - \sec^2\alpha_2) \tag{31}$$

$$\therefore \quad \frac{\triangle P^1}{\tfrac{1}{2}\,\varrho\,.\,V_a^2\sec^2\alpha_1} = 1 - \frac{\sec^2\alpha_2}{\sec^2\alpha_1}$$

$$\therefore \quad \frac{\triangle P^1}{\tfrac{1}{2}\,\varrho\,.\,V_1^2} = 1 - \frac{\cos^2\alpha_1}{\cos^2\alpha_2}$$

The efficiency of the blade row $\eta_B = \dfrac{\triangle P^1 - \overline{\omega}}{\triangle P^1} = 1 -$

$$\frac{\dfrac{\overline{\omega}}{\tfrac{1}{2}\,\varrho\,.\,V_1^2}}{\dfrac{\triangle P^1}{\tfrac{1}{2}\,\varrho\,.\,V_1^2}} \tag{32}$$

With 50% reaction blading this formula will hold good for both stator and rotor blade rows.

Also $\eta_B = \dfrac{P_2 - P_1}{P_2^1 - P_1}$

The stage efficiency η_s is the ratio isentropic temperature rise/actual temperature rise.

$$\frac{P_2}{P_1} = \left[1 + \frac{\eta_s \triangle Ts}{2T_1}\right]^{\frac{y}{y-1}}$$

$\dfrac{\triangle Ts}{2}$ being the temperature rise in the rotor for 50% reaction.

$$\therefore \quad \frac{P_2^1}{P_1} = \left[1 + \frac{\triangle Ts}{2T_1}\right]^{\frac{y}{y-1}} \quad \therefore \quad \eta_B = \frac{\dfrac{P_2}{P_1} - 1}{\dfrac{P_2^1}{P_1} - 1}$$

$$= \frac{\left[1 + \frac{\eta_s \triangle Ts}{2T_1}\right]^{\frac{y}{y-1}} - 1}{\left[1 + \frac{\triangle Ts}{2T_1}\right]^{\frac{y}{y-1}} - 1}$$

$$= \eta_s \left[1 - \frac{1}{y-1} \cdot \frac{\triangle Ts}{4T_1} (1 - \eta_s) \right] \quad (34)$$

In present day power plants $\triangle T_s$ would be approximately 35°C. and T_1 about 288°K. at the first stage thus the second term in the bracket can be disregarded giving :—

$$\eta_B = \eta_s$$

In the case of the half vortex case an approximate stage efficiency is evolved by taking the arithmetic mean of the efficiencies of the two blade rows.

$$\eta_s = \tfrac{1}{2} (\eta_B \text{ Rotor} + \eta_s \text{ Stator}) \quad (35)$$

When the degree of reaction is considerably removed from 50% reaction a more accurate expression for the stage efficiency would be :—

$$\eta_s = \wedge \cdot \eta_B \text{ Rotor} + (1 - \wedge) \cdot \eta_s \text{ Stator} \quad (36)$$

The degree of reaction $\wedge$ being obtained from equation (25).

Characteristics at High Speed.

The critical condition at any point in a blade passage is when the velocity of the air exceeds that of the local speed of sound, which causes shock waves and a loss in total head pressure. The velocity of sound in air increases with rising temperatures thus the Mach numbers in a compressor will decrease progressively through the stages. On this basis the early stages are the most critical and the worst condition is when the compressor is operating at altitude.

$$M_1 = \frac{V_1}{(y \cdot g \cdot R \cdot T_1)^{\frac{1}{2}}} \quad (37)$$

The performance falls after the Mach number reaches 0·7 and gradually increases until the flow chokes at the minimum cross section. The critical and maximum Mach numbers are M_{1c} and M_{1m} respectively. A loss of about 5% occurs midway between M_{1c} and M_{1m} after which the loss increases considerably. Fig. 8 illustrates the effect of Mach numbers on the pressure rise of a cascade of blades.

Design Method.

Certain generalised design curves have been evolved, and are helpful to the designer in fixing certain arbitrary figures.

Example.

Design an axial flow compressor given the following data :—

Q = 50 lb. per sec.
T_1 = 288°K.
P_1 = 14·7 lb. per sq. in.
R.P.M. = 12,000.
Ω = 0·86.
No. of Stages = 12.
ΔT_s = 35°C.
Type of blading = 50% Reaction.
V_a = 600 ft. per sec.
Tip diameter of compressor = 18 ins.

The entry annulus is determined from the equation of continuity.

$$A = \frac{Q}{V_a \times \varrho} \quad \text{where } \varrho_1 = \frac{P_1}{R \times T_1} \quad \therefore \varrho_1 = \frac{14{\cdot}7 \times 144}{96 \times 288}$$

$$= 0{\cdot}0765 \text{ lb. per cu. ft.}$$

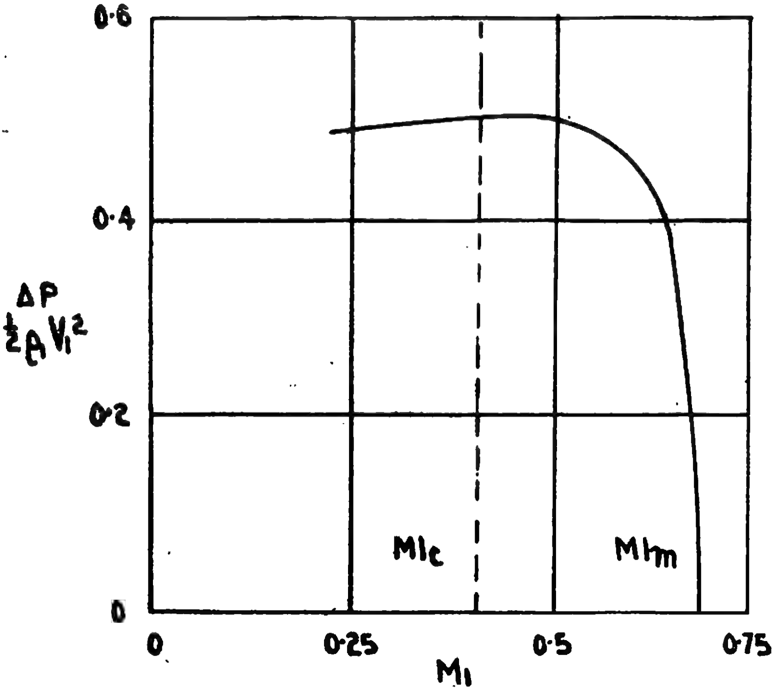

Fig. 8—Effect of Mach. Number MI on the Pressure Rise in a Cascade of Compressor Blades.

$$A = \frac{50}{600 \times 0{\cdot}0765} = 1{\cdot}090 \text{ sq. ft.}$$

Also $A = \pi/4\ (D^2 - d^2)$ from which $d = \sqrt{\frac{1{\cdot}090 \times 144}{0{\cdot}7854} + 18^2}$

$$= 11{\cdot}180.$$

Height of blade at entry $= \frac{18{\cdot}000 - 11{\cdot}180}{2} = \frac{6{\cdot}820}{2} = 3{\cdot}410$ ins.

From equation (20) $(\tan \alpha_1 - \tan \alpha_2) = \frac{\Delta T_{st}}{\Omega\, 0{\cdot}923\ (U/100)\ (V_a/100)}$

where U is velocity.

At the mean radius $U = \frac{12{,}000\ .\ \pi\ .\ 14{\cdot}590}{60\ .\ 12} = 763$ ft./sec.

$$\therefore\ (\tan \alpha_1 - \tan \alpha_2) = \frac{25{\cdot}88}{0{\cdot}923\ .\ 7{\cdot}63\ .\ 6\ .\ 0{\cdot}86} = 0{\cdot}712.$$

For 50% reaction $\Lambda = \frac{1}{2} \times Va/U\ (\tan \alpha_1 + \tan \alpha_2)$ (38)

$$\therefore\ 0{\cdot}5 = \tfrac{1}{2}\ .\ \frac{600}{763}\ (\tan \alpha_1 + \tan \alpha_2).$$

Whence $(\tan \alpha_1 + \tan \alpha_2) = \frac{763}{600} = 1{\cdot}272.$

$\tan \alpha_1 - \tan \alpha_2 = 0{\cdot}712.$
$\tan \alpha_1 + \tan \alpha_2 = 1{\cdot}272.$

Subtracting	$-2 \tan \alpha_2$	$= -0{\cdot}560$
Adding	$2 \tan \alpha_1$	$= 1{\cdot}984$

$\tan \alpha_1 = \frac{1{\cdot}984}{2} = 0{\cdot}992 \quad \therefore\ \alpha_1 = 44°\ 47'$

$\tan \alpha_2 = \frac{-0{\cdot}560}{-2} = 0{\cdot}280 \quad \therefore\ \alpha_2 = 15°\ 39'$

Since there is 50% reaction $\alpha_0 = \alpha_2 = 15°\ 39'$

$\alpha_3 = \alpha_1 = 44°\ 47'$

These angles occur at the mean radius r_m and it is now necessary to obtain variations of these angles over the total blade height.

Assuming that axial velocity and work input per lb. are constant with radius

$$Va = \text{constant } (K_1) \quad (39)$$

D

and work done per lb. of air per sec., $W = U/g\,(V_{w3} - V_{wa})$ ft. lb. (40)
where V_{wa} and V_{w3} are the whirl components of the absolute velocities of the air at the inlet to and exit from the rotor.

From equation (40) $U_r\,(V_{w3} - V_{wo}) = Ur\,.\,V_a\,(\tan \alpha_3 - \tan \alpha_o)$
$= \text{constant } (K_2)$ (41)

Where Ur = peripheral velocity at any radius $r = U \times r$ (42)

In order to simplify the calculation $r = 1$.

$$\text{Now } \frac{Ur}{Va} = \tan \alpha_1 + \tan \alpha_o = \tan \alpha_2 + \tan \alpha_3 \tag{43}$$

From equations (41) and (42) $U\,.\,r\,.\,K_1\,(\tan \alpha_3 - \tan \alpha_o) = K_2$,

$$\text{or } (\tan \alpha_3 - \tan \alpha_o) = \frac{K_2}{U\,.\,r\,.\,K_1} \tag{44}$$

$$\text{From equation (43) } \tan \alpha_1 + \tan \alpha_o = \frac{U\,.\,r}{K_1} \tag{45}$$

$$\text{and } \tan \alpha_2 + \tan \alpha_3 = \frac{U\,.\,r}{K_1} \tag{46}$$

$$\text{From the theory of free vortex } V_{wo} = \frac{\text{constant}}{r}$$

$$\therefore\ Va \tan \alpha_o = \frac{\text{constant}}{r}$$

$$\text{hence } \tan \alpha_o = \frac{K_3}{r}$$

Substituting this in equations (44) and (45) we get :—

$$\tan \alpha_3 = \frac{K2}{U\,.\,r\,.\,K_1} + \frac{K3}{r}$$

$$\text{and } \tan \alpha_1 = \frac{U\,.\,r}{K_1} - \frac{K3}{r}$$

assuming 50% reaction at the design radius $r = 1$.

$$\tan \alpha_1 = \tan \alpha_3 \text{ when } r = 1.$$

$$\therefore\ \frac{K_2}{U\,.\,K_1} + K_3 = \frac{U}{K_1} - K_3$$

$$\text{From which } \tan \alpha_o = \frac{U - \dfrac{K_2}{U}}{2K_1\,.\,r} \tag{47}$$

$$\tan \alpha_1 = \frac{U \, . \, r}{K_1} - \frac{U - \dfrac{K_2}{U}}{2K_1 \, . \, r} \tag{48}$$

$$\tan \alpha_3 = \frac{K_2}{U \, . \, r \, . \, K_1} + \frac{U - \dfrac{K_2}{U}}{2K_1 \, . \, r} \tag{49}$$

$$\tan \alpha_2 = \frac{U \, . \, r}{K_1} - \frac{U + \dfrac{K_2}{U}}{2K_1 \, . \, r} \tag{50}$$

For constant 50% reaction at all radii :—

$$\tan \alpha_1 = \tan \alpha_3 = \tfrac{1}{2}\left[\frac{U \, . \, r}{K_1} + \frac{K_2}{U \, . \, K_1 \, . \, r}\right] \tag{51}$$

$$\tan \alpha_0 = \tan \alpha_2 = \tfrac{1}{2}\left[\frac{U \, . \, r}{K_1} - \frac{K_2}{U \, . \, K_1 \, . \, r}\right] \tag{52}$$

$$\left\{\begin{array}{lll} K_1 & = Va = 600 & \\ K_2 & = U \, . \, Va \, (\tan \alpha_1 - \tan \alpha_2) & = 763{\cdot}600 \; (0{\cdot}712) \\ & & = 325{\cdot}953. \end{array}\right.$$

We can now obtain the air angles α_1, α_3 and α_o, α_2 over the entire annulus. The air angle distributions are shown graphically in Fig. 9.

From equation (11) $\epsilon^* = 0{\cdot}8\,(29^\circ\ 08') = 23^\circ\ 18'$ and from Design

Deflection Curves S/C = 1·1 (see Fig. 10) obtained from cascade tests.

Substituting in equation (12) $\delta = \left[0{\cdot}23 + 0{\cdot}1\,\dfrac{15{\cdot}65}{50}\right]\sqrt{1{\cdot}1}\,.\,\theta$

$$= 0{\cdot}275\,\theta$$

Now $\theta = \beta_1 - \beta_2$ and $\beta_2 = \alpha_2 - \delta$

$\therefore\ \theta = \beta_1 - (\alpha_2 + \delta) = \beta_1 - \alpha_2 + 0{\cdot}275\,\theta$

$i = \alpha_1 - \beta_1 = 2{\cdot}2^\circ$ (obtained from cascade)

$\therefore\ \beta_1 = 44^\circ\ 47' - 2^\circ\ 12' = 42^\circ\ 35'$

$\therefore\ \theta = 42^\circ\ 35' - \alpha_2 + 0{\cdot}275\,\theta$

$\therefore\ 0{\cdot}725\,\theta = 42^\circ\ 35' - 15^\circ\ 39' = 26^\circ\ 56'$

$\therefore\ \theta = 37^\circ\ 45'$ and $\beta_2 = \beta_1 - \theta = 4^\circ\ 50'$

Also $\zeta = \beta_1 - \theta/2 = 42^\circ\ 35' - 18^\circ\ 52' = 23^\circ\ 43'$

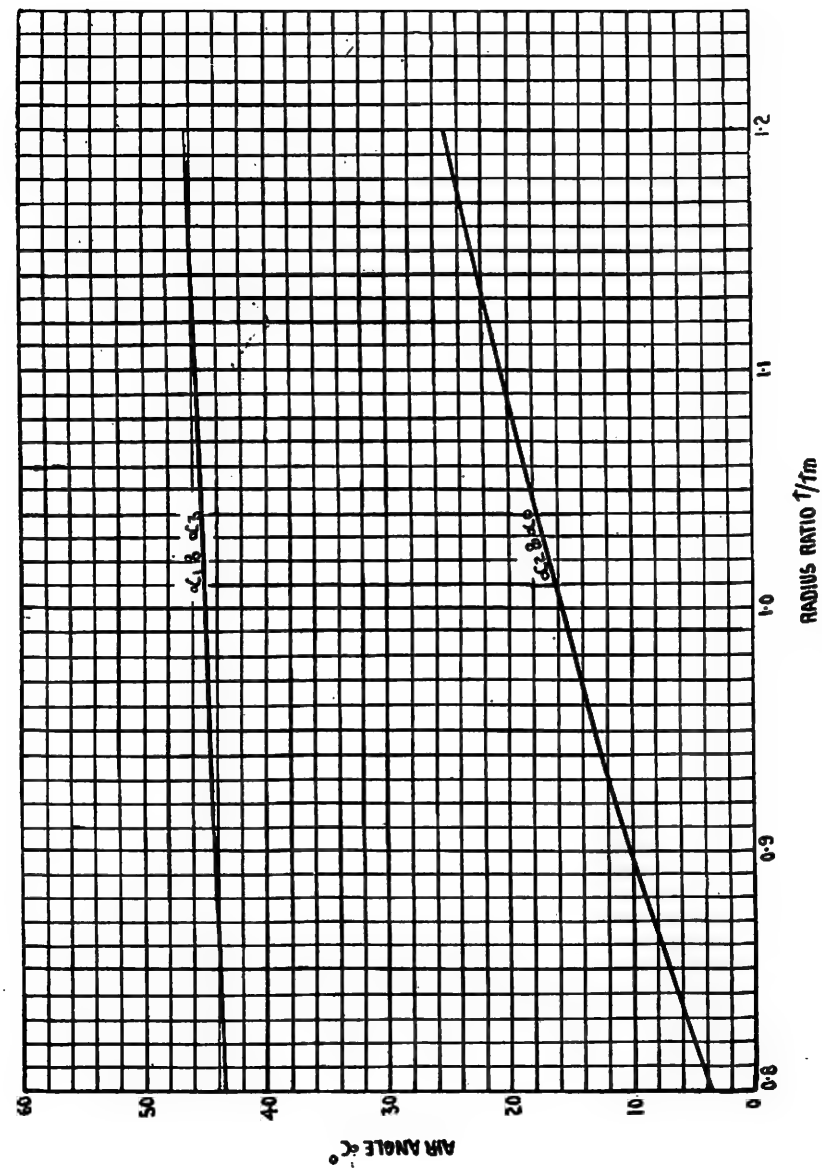

Fig. 9—Air Angle Distributions—Constant Reaction.

Assuming that there are 42 blades in a row, at r_m :—

$$S = \frac{2 \times 7{\cdot}295}{42} = 1{\cdot}090$$

$$C = \frac{S}{1{\cdot}1} = \frac{1{\cdot}090}{1{\cdot}1} = 0{\cdot}99$$

$$\text{Aspect ratio} = \frac{h}{c} = \frac{3{\cdot}410}{0{\cdot}990} = 3{\cdot}450$$

This process has now to be repeated at selected points along the blade length. The S/C ratio is derived from the corresponding air angles and the chordal length is determined thus a complete picture of the blade is obtainable. The following table gives the complete data for the stage in question.

r/r_m	α_1	α_2	β_1	β_2	θ	ζ	S	C	S/C	h/c
0·8	43° 36′	3° 40′	41° 18′	-6° 27′	47° 45′	17°. 26′	0·873	1·091	0·8	3·125
1·0	44° 47′	15° 39′	42° 35′	4° 50′	37° 45′	23° 41′	1·090	0·99	1·1	3·450
1·2	46° 38′	25° 1′	44° 26′	14° 56′	29° 30′	29° 41′	1·309	0·872	1·5	3·910

Adopting a Gottingen 436 aerofoil section, Fig. 11 illustrates the velocity diagrams and blade layout for the mean radius position.

Drag and Lift Co-efficients.

From equation (6) $\tan \alpha_m = \frac{1}{2}(\tan 44° 47' + \tan 15° 39') = \frac{1}{2}(0{\cdot}9924 + 0{\cdot}2801) = \frac{1}{2} . 1{\cdot}2725 = 0{\cdot}6362 \quad \therefore \alpha_m = 32° 28'$.

From equation (10) $C_L = 2 . 1{\cdot}1 (0{\cdot}7123)\ 0{\cdot}8437 = 2{\cdot}2 . 0{\cdot}7123 . 0{\cdot}8437 = 1{\cdot}325$.

Hence from equation (26) $C_{DS} = 0{\cdot}018 (1{\cdot}325)^2 = 0{\cdot}0315$

At this radius $S = 1{\cdot}090$ and $h = 3{\cdot}410$ $\therefore$ from equation (27)

$$C_{DA} = 0{\cdot}020 . \frac{1{\cdot}090}{3{\cdot}410} = 0{\cdot}006$$

The variation of the profile drag co-efficient C_{DP} is comparatively narrow for a wide range of geometrical forms of cascade and a constant value of 0·018 has been adopted.

$$\therefore \quad C_D = C_{DP} + C_{DS} + C_{DA} = 0{\cdot}018 + 0{\cdot}031 + 0{\cdot}006 = 0{\cdot}055$$

From equation (28) $\dfrac{\overline{\omega}}{\frac{1}{2}\rho . V_1^2} = C_D \div s/c \, . \dfrac{\cos^3 \alpha_m}{\cos^2 \alpha_1}$

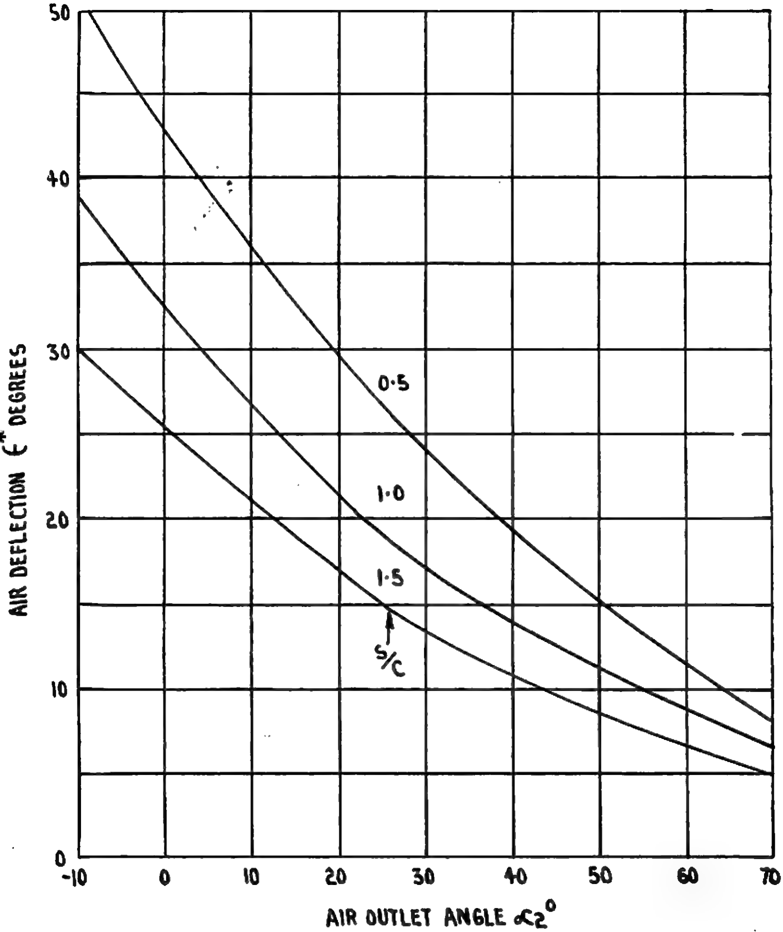

Fig. 10—Design Deflection Curves.

$$= \frac{0{\cdot}055}{1{\cdot}1} \quad \frac{\cos^3 19^\circ\ 36'}{\cos^2 44^\circ\ 47'} = 0{\cdot}0596$$

From equation (3) the theoretical pressure rise through the blade row is found by putting the loss $\overline{\omega}$ equal to zero, which gives :—

$$\triangle Pth = \tfrac{1}{2}\,\varrho\, Va^2\,(\tan^2 \alpha_1 - \tan^2 \alpha_2) = \tfrac{1}{2}\,\varrho\, Va^2\,(\sec^2 \alpha_1 - \sec^2 \alpha_2).$$

$$\therefore \frac{\triangle Pth}{\frac{1}{2}\varrho\, Va^2 \sec^2\alpha_1} = 1 - \frac{\sec^2\alpha_2}{\sec^2\alpha_1} \quad i.e., \quad \frac{\triangle Pth}{\frac{1}{2}\,\varrho\, V_1^2} = 1 - \frac{\cos^2\alpha_1}{\cos^2\alpha_2}$$

$$= 1 - \frac{0{\cdot}503}{0{\cdot}927} = 0{\cdot}458.$$

From equation (32) $\eta_B = 1 - \dfrac{0{\cdot}0596}{0{\cdot}458} = 1 - 0{\cdot}130 = 87\%.$

Substituting static temperatures in equation (21) we get

$$Rs = \left(1 + \frac{\eta s\,.\,\triangle Ts}{T_1}\right)^{\frac{y}{y-1}} = \left(1 + \frac{0{\cdot}870\,.\,25{\cdot}88}{288}\right)^{3{\cdot}5}$$

$$= (1{\cdot}0782)^{3{\cdot}5} = 1{\cdot}3015.$$

Overall Performance.

The overall static pressure ratio $R = \dfrac{P_2}{P_1} = \left(\dfrac{T_2}{T_1}\right)^{\frac{n}{n-1}}$

$$= \left(\frac{T_2}{T_1}\right)^{\eta s \frac{y}{y-1}} \qquad (53)$$

We have assumed that $T_1 = T_a$ where T_a = the ambient temperature, but in fact it will be less than T_a due to the temperature equivalent of the air velocity at the mean radius. This velocity is V_o (see Fig. 7).

Temperature equivalent of $V_o = \dfrac{(V_a \sec\alpha_o)^2}{2g\,.\,J\,.\,Cp} = \dfrac{(600 \sec 15^\circ\ 39')^2}{21{,}638}$

$$= 17{\cdot}9^\circ C.$$

$T_1 = 288 - 17{\cdot}9 = 270{\cdot}1^\circ$ K.

$$\therefore\ R_s = \left(1 + \frac{0{\cdot}87\,.\,25{\cdot}88}{270{\cdot}1}\right)^{3{\cdot}5} = (1{\cdot}0834)^{3{\cdot}5} = 1{\cdot}3236.$$

Assuming V_a is constant throughout the compressor

$T_2 - T_1 = 12 \times 25{\cdot}88 = 310{\cdot}56^\circ K.$

$\therefore\ T_2 = 310{\cdot}56 + 270{\cdot}10 = 580{\cdot}66^\circ K.$

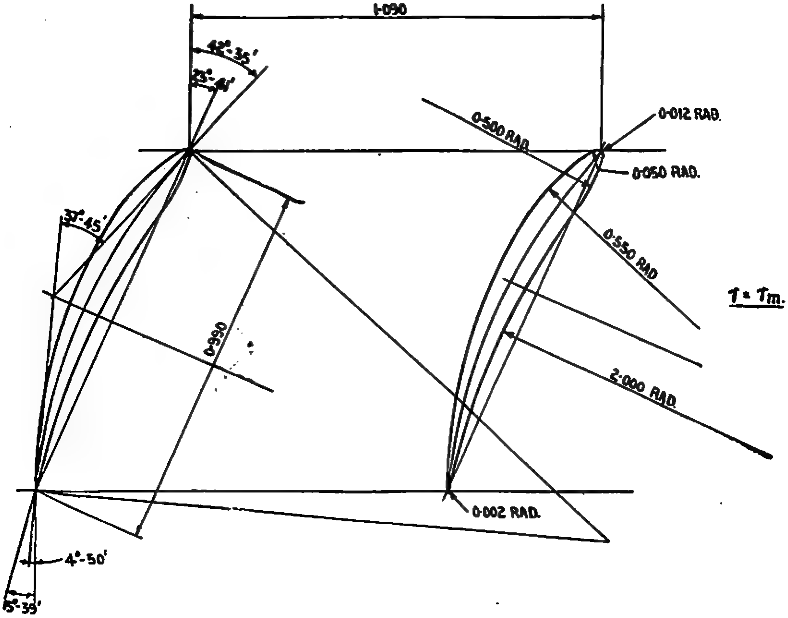

Fig. 11—Layout of Compressor Blading.

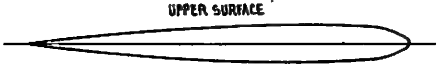

ORDINATES FOR 10% THICKNESS

% CHORD	UPPER SURFACE	LOWER SURFACE
1·25	1·49	1·63
2·5	2·08	2·26
5·0	3·0	3·12
7·5	3·58	3·66
10·0	4·01	4·06
15·0	4·55	4·58
20·0	4·90	4·91
30·0	4·98	5·02
40·0	4·76	4·79
50·0	4·30	4·31
60·0	3·70	3·72
70·0	2·91	3·00
80·0	2·02	2·15
90·0	1·05	1·20
95·0	0·60	0·68

LEADING EDGE RAD. 1·2 TRAILING EDGE RAD. 0·2

From equation (53) $$\frac{P_2}{P_1} = \left(\frac{580\cdot66}{270\cdot10}\right)^{0\cdot87\,.\,3\cdot5} = \left(\frac{580\cdot66}{270\cdot10}\right)^{3\cdot045}$$
$$= 10\cdot283.$$

Compressibility Effects.

The relative velocity V_1 at the mean radius at the first stage is given by :—

$$V_1 = V_a \sec \alpha_1 = 600 \times 1\cdot4088 = 845\cdot28 \text{ ft./sec.}$$

$$\therefore \quad M = \frac{845}{\sqrt{32\cdot2 \times 1\cdot4 \times 96 \times 270\cdot10}} = \frac{845}{1170} = 0\cdot781.$$

This figure is quite satisfactory.

CENTRIFUGAL COMPRESSOR DESIGN FOR AIRCRAFT ENGINES.

The rapid development of gas turbines during the war resulted in the majority of aero-engine manufacturers adopting the centrifugal compressor rather than its axial counterpart. Previous design experience with superchargers, based on centrifugal principles no doubt influenced this trend. High delivery pressures were initially not required as total thrust was not of such a high order as it is to-day and weight was an important factor as was total length. All these factors resulted in the centrifugal compressor being favoured as a means to secure adequate compression.

Three types of impeller vanes are possible, namely, the back swept vane, the straight radial vane and the forward swept vane. The three types are illustrated in Fig. 1. The back swept and straight radial types are in common use, but the forward swept type is not used, despite the fact that it gives the highest pressure-ratio. Its chief drawback lies in the excessive diffuser losses, due to the considerable absolute air velocity leaving the impeller.

In comparing the straight radial with the backward curved type it can be seen that the straight radial vane is a particular case of the curved backward vane in which the blade entry and outlet angles are equal. Therefore any calculations for one type are applicable to the other, provided allowances are made for the differences in vane angles.

Nomenclature.

V_{a_1} = Absolute velocity of entry air in feet per second.
V_1 = Velocity of entry air relative to impeller in ft./sec.
V_{w_2} = Whirl velocity in feet per second.
U = Tangential velocity of impeller tip in feet per second.
V_2 = Absolute velocity of outlet air in feet per second.
U_2 = Velocity of outlet air relative to impeller in ft./sec.
U_1 = Tangential velocity of blade edges at entry in ft./sec.
ω = Angular velocity of impeller in radians per second.
V_{a2} = Absolute velocity of entry air with prewhirl in ft./sec.
V_{r2} = Radial velocity in feet per second.
σ = Slip factor.
r_1 = Radius of entry annulus in feet.
r_2 = Radius of impeller in feet.
p = Power input factor.
Q = Mass flow of air.
T_{1t} = Inlet total-head temperature.
P_{1t} = Inlet total-head pressure.

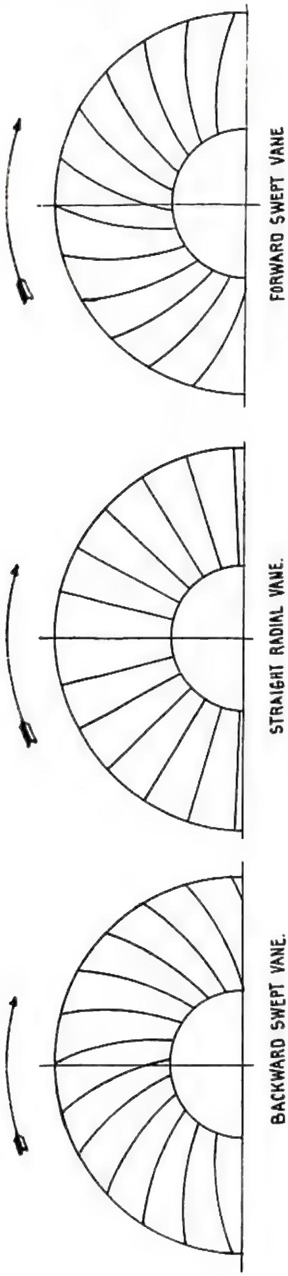

Fig. 1—Types of Impellers.

T_{2t} = Outlet total-head temperature.
P_{2t} = Outlet total head pressure.
y = Ratio of specific heats $\frac{C_p}{C_v}$
η_c = Isentropic efficiency of compressor.
α_1 = Vane inlet angle.
C_p = Specific heat at constant pressure.
C_v = Specific heat at constant volume.

Compressors can be single or double-sided as shown in Fig. 2. (*a*) and (*b*) or should higher compression ratios be required they

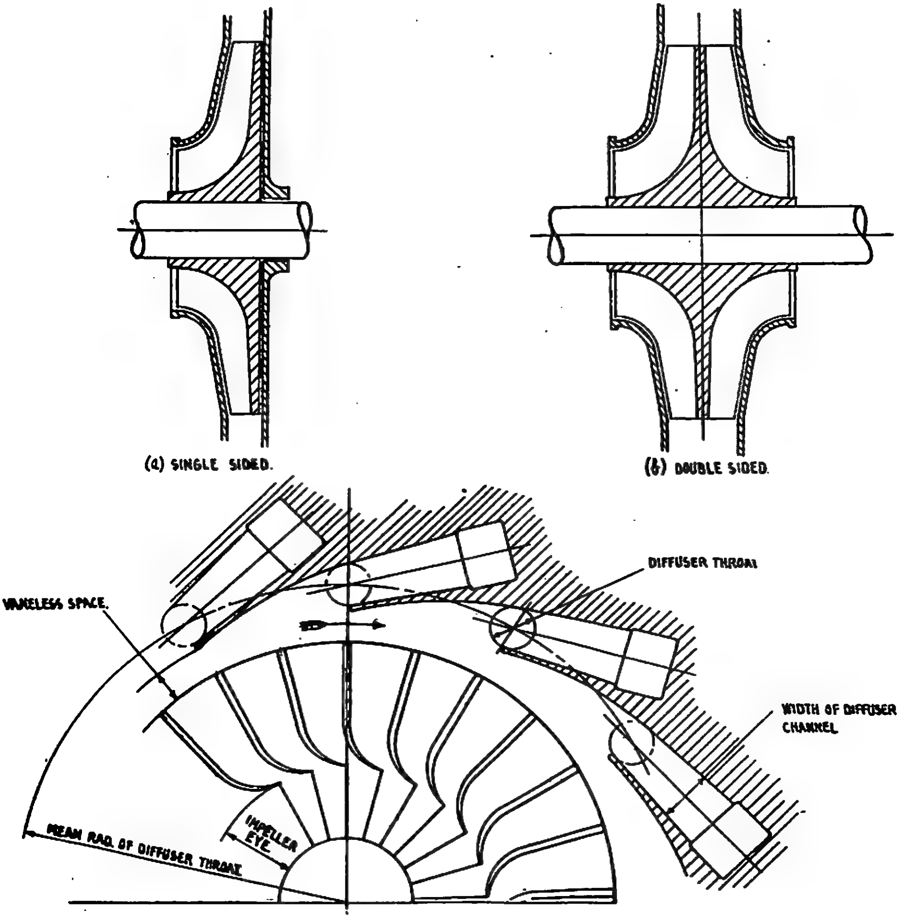

Fig. 2—Centrifugal Compressors.

can be of the compounded type. Basically their fundamental theory is the same. The majority of modern centrifugal compressors are of the straight radial type.

Air is sucked into the impeller eye at an absolute velocity V_{a_1} and a relative velocity V_1 is whirled at a peripheral speed U and flung out by centrifugal force at an absolute velocity V_2 and relative velocity U_2. The centripetal acceleration is obtained by a pressure head, therefore the static pressure of the air increases from eye to tip of impeller. The kinetic energy of the air is now converted into pressure energy by means of a diffuser by which the final velocity of the air is reduced to somewhere in the region of the velocity with which the air originally entered the impeller eye.

Work Done During Compression.

Fig. 3 illustrates a typical centrifugal compressor with the necessary nomenclature employed. It can be seen that the incoming air has an initial velocity of V_{a_1} and that it possesses no angular momentum. In order that the air can pass smoothly into the vanes, the axial portion between the eye root and eye tip must be curved. This inlet angle α_1 will be given by the direction of the relative velocity V_1.

Under the action of centrifugal force the air leaves the tip of the impeller with an absolute velocity V_2 and a tangential or whirl velocity V_{w_2} together with a small radial component V_{r_2}. Under the ideal conditions the velocity V_2 would be such that the whirl velocity $V_{w_2} = U$, the tangential speed of the impeller tip. However, due to the reluctance of the air trapped between the vanes to move round, with the impeller, the static pressure on the leading face of the vane exceeds that of the trailing edge so that the air is prevented from acquiring a whirl velocity equal to the impeller speed. This phenomenon is called "slip" and its amount is largely dependent upon the number of vanes in the impeller. In practice this figure is smaller when the number of vanes are increased and it is necessary in the course of design to assume a value for σ where

σ is the ratio $\dfrac{V_{w_2}}{U}$

Considering a flow of 1 lb. of air per second through the impeller the theoretical torque is equal to the rate of change of angular momentum and is given by :—

$$\text{Theoretical torque} = \frac{V_{w_2} \times r_2}{g} \text{ lb. ft.} \qquad (1)$$

If the angular velocity is radians per second is ω the work done on 1 lb. of air per second will be :—

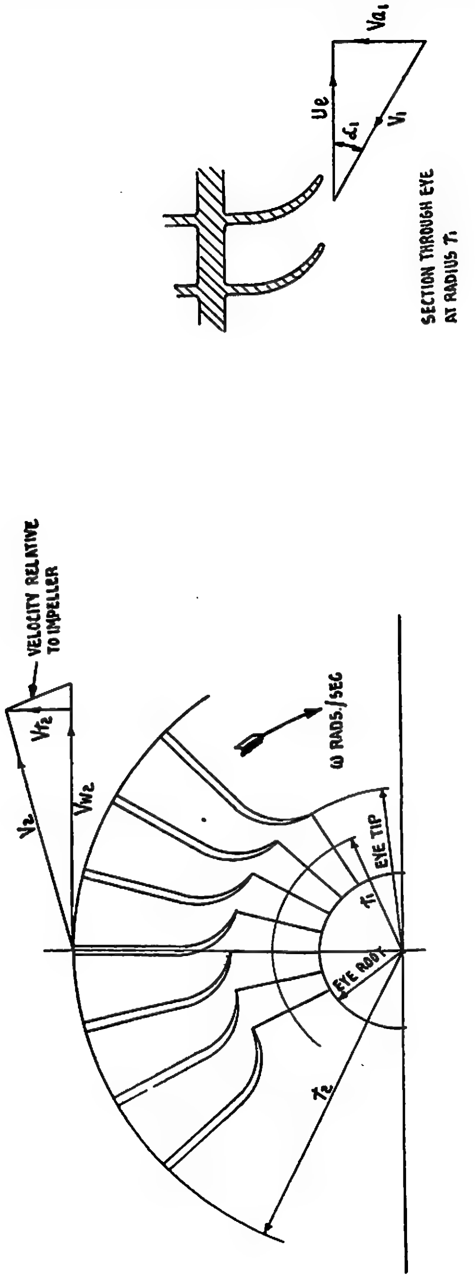

Fig. 3—Compressor Nomenclature.

$$\frac{V_{w_2} \times r_2 \times \omega}{g} = \frac{V_{w_2} \times U}{g} \text{ ft. lb. per sec.} \qquad (2)$$

When introducing the slip factor, theoretical work done

$$\frac{\sigma\, U^2}{g} \text{ ft. lb. per second.}$$

During the passage of the air through the vanes, certain losses occur such as friction, etc., which result in the actual work input being greater than the theoretical value given in (2). To compensate for this a "power input factor" is introduced so that the actual work done on the air becomes

$$\frac{p \times \sigma \times U^2}{g} \text{ ft. lb. per second} \qquad (3)$$

If Q. lb. of air per second are passing through the impeller then the total work done per second by the impeller is

$$Q \times \frac{p \times \sigma \times U^2}{g} \text{ ft. lbs./sec.}$$

and the horse-power equivalent of the work done on the air is

$$Q \times \frac{p \times \omega \times U^2}{550\, g} \qquad (4)$$

Pressure Rise.

The work done on the air during compression can be considered in terms of temperature changes across the whole compressor. Ideally the type of compression should be isentropic (*i.e.*, reversible adiabatic) but due to the friction of the air passing through the vane channels, a perfect isentropic compression cannot be obtained hence the introduction of the power input factor.

The difference between the power input factor and the slip factor should be clearly understood. Introducing the power input factor represents the increase in total work input due to overcoming frictional losses which results in the raising of the outlet temperature. It then follows that the maximum cycle temperature can be reached without burning so much fuel, hence these losses are not entirely wasted. Thus we can still adopt the isentropic type of compression for calculation purposes, bearing in mind that the power input factor should be kept as low as possible. Present day designs require that this factor should be between 1·030 to 1·040.

The slip factor is the ratio $\frac{V_{w_2}}{U}$ and it can be seen from the velocity triangles in Fig. 3 and its introduction into formulae

determining total work decreases this figure. It will be clearly seen that the nearer V_{w_2} reaches the value U the greater the total work done. Increasing the number of vanes in the impeller would appear to increase σ, but in doing so the effective flow area of the impeller eye is decreased. Greater frictional losses thus occur, since for the same mass flow the inlet velocity must be increased. A compromise has been found by experimental means whereby a suitable number of vanes will give a slip factor of 0·9, *i.e.*, about 25 vanes.

Now the temperature equivalent of the work done on the air given by equation (3)

$$= \frac{p \times \sigma \times U^2}{g \times J \times Cp} \qquad (5)$$

where Cp is the mean specific heat over the temperature range $T_{2t} - T_{1t}$, which is the total-head temperature rise across the impeller. It therefore follows that :—

$$(T_{2t} - T_{1t}) = \frac{p \times \sigma \times U^2}{g \times J \times Cp} \qquad (6)$$

Also work done $= Q\ J\ Cp\ (T_{2t} - T_{1t})$ ft. lb./sec. (7)

$$\therefore \text{ Horse-power equivalent} = \frac{Q \times J \times Cp}{550}(T_{2t} - T_{1t}) \qquad (8)$$

Adiabatic Efficiency.

If a value be assumed for the total-head isentropic efficiency, ηc, then we know how much of the work is actually used to compress the air. Thus the total-head pressure ratio may be found as follows :—

$$\frac{P_{2t}}{P_1t} = \frac{(T_{2t}^1)}{T_1t}^{\frac{y}{y-1}} = \left[1 + \eta c \frac{(T_2t - T_1t)}{T_1t}\right]^{\frac{y}{y-1}}$$

$$= \left[1 + \eta c \times \frac{p \times \sigma \times U^2}{g \times J \times Cp \times T_1t}\right]^{\frac{y}{y-1}} \qquad (9)$$

From equation (9) it will be seen that the factors influencing the pressure ratio are the power input factor p, the slip factor σ, the impeller tip speed U and the total-head inlet temperature T_1t. A well-designed centrifugal compressor when running under near perfect conditions can achieve an efficiency of 75% - 80%. Very little energy is actually lost during compression but quite a con-

siderable portion of the energy goes into heating the air to a temperature higher than that which would be obtained from a perfect isentropic compression.

The ideal temperature rise corresponds to a perfect isentropic compression, *i.e.*, $T_2t^1 - T_1t$, and if the actual total head temperature rise is $T_2t - T_1t$ then it follows that :—

$$\eta c \quad = \quad \frac{T_2t^1 - T_1t}{T_2t - T_1t} \tag{10}$$

$$= \quad \frac{T_1t \left[\left(\frac{P_2t}{P_1t}\right)^{\frac{y-1}{y}} - 1 \right]}{T_2t - T_1t} \tag{11}$$

Sometimes it is convenient to express the isentropic efficiency in terms of pressure-ratio, which can be done in the following manner :—

Work required for perfect isentropic compression is given by the expression :—

$$Q \times J \times Cp \ (T_2t^1 - T_1t) \text{ ft. lbs. per second.}$$

and the actual work required to effect the compression is given by the expression :—

$$Q \times J \times Cp \ (T_2t - T_1t) \text{ ft. lbs. per second.}$$

$$\text{But} \quad T_{2t}{}^1 \quad = \quad T_1t \quad \left(\frac{P_2t}{P_1t}\right)^{\frac{y-1}{y}}$$

$$\text{and} \quad T_2t \quad = \quad T_1t \quad \left(\frac{P_2t}{P_1t}\right)^{\frac{n-1}{n}}$$

Substituting these values into expressions for work done :—

$$\text{Isentropic work} \quad = \quad Q \times J \times Cp \times T_1t \left[\left(\frac{P_2t}{P_1t}\right)^{\frac{y-1}{y}} - 1 \right]$$

$$\text{Actual work} \quad = \quad Q \times J \times Cp \times T_1t \left[\left(\frac{P_2t}{P_1t}\right)^{\frac{n-1}{n}} - 1 \right]$$

Since the isentropic efficiency is the ratio :—

$$\frac{\text{isentropic work}}{\text{actual work}}$$

then

$$\eta c = \frac{\left(\frac{P_2t}{P_1t}\right)^{\frac{\gamma-1}{\gamma}} - 1}{\left(\frac{P_2t}{P_1t}\right)^{\frac{n-1}{n}} - 1} \qquad (12)$$

Denoting the pressure-ratio $\frac{P_2t}{P_1t}$ by r the expression (12) becomes

$$\eta c = \frac{r^{\frac{\gamma-1}{\gamma}} - 1}{r^{\frac{n-1}{n}} - 1} \qquad (13)$$

Theoretically, it is very difficult to obtain the value of n and therefore recourse should be made to the data obtained from tests carried out on previous compressors.

We will now consider the design of a double sided centrifugal compressor having been given the following data :—

Overall diameter of impeller	21 ins.
Eye tip diameter	12 ins.
Eye root diameter	6·5 ins.
Total mass flow Q	40 lb. per second
Power input factor p	1·040
Slip factor σ	0·90
Revs. per minute	15,000
Inlet total temperature T_1	288°K
Inlet total pressure P_1	14·7 lbs. per sq. in.
Total head isentropic efficiency	76%
Density of inlet air ϱ	0·0765 lb./cu. ft.

$$U = \frac{15000 \times 21 \times \pi}{60 \times 12} = 1371 \text{ ft. per sec.}$$

From (6) $$T_2t - T_1t = \frac{1{\cdot}04 \times 0{\cdot}9 \times 1371^2}{32{\cdot}2 \times 1400 \times 0{\cdot}24} = 162{\cdot}6°\text{C.}$$

$$T_{2t_1} - T_{1t} = 0{\cdot}76 \times 162{\cdot}6 = 123{\cdot}6°\text{C.}$$

From (8) H.P. required $$= \frac{40 \times 1400 \times 0{\cdot}24 \times 162{\cdot}6}{550} = 3973 \text{ H.P.}$$

The inlet velocity which is axial is not known and in order to determine the inlet angle of the vanes it is necessary to satisfy the equation of continuity $Q = \varrho_1 \times A \times Va_1$, and it is assumed that the mass flow is equally divided between both sides of the impeller.

$$A = \frac{\pi\,(12^2 - 6{\cdot}5^2)}{4 \times 144} = 0{\cdot}555 \text{ sq. ft.}$$

The equation of continuity $Q = A \times V_{a_1} \times \varrho$ as $\varrho = 0{\cdot}0765$.

$$\therefore \quad 20 = 0{\cdot}0765 \times 0{\cdot}0555 \times V_{a_1} \text{ whence } V_{a_1} = \frac{20}{0{\cdot}0765 \times 0{\cdot}555}$$

$$= 469{\cdot}4 \text{ ft. per sec.}$$

The inlet total head temperature $T_{1t} = T_1 + \dfrac{Va_1^{\,2}}{2g \times J \times Cp}$

$$= 288^\circ + \frac{469{\cdot}4^2}{64{\cdot}4 \times 1400 \times 0{\cdot}24}$$

$$= 288^\circ K + 10{\cdot}2^\circ C = 298{\cdot}2^\circ K$$

Now $\dfrac{P_{1t}}{P_1} = \left(\dfrac{T_1t}{T_1}\right)^{\frac{\gamma}{\gamma-1}}$ Hence $P_{1t} = 14{\cdot}7 \times \left(\dfrac{298{\cdot}2}{288}\right)^{3\cdot5}$

$$= 14{\cdot}7 \times 1{\cdot}125 = 16{\cdot}5 \text{ lb. per sq. in.}$$

From (9) $\dfrac{P_2t}{P_1t} = \left[1 + \dfrac{123{\cdot}6}{298{\cdot}2}\right]^{3\cdot5} = 3{\cdot}366$

The peripheral speed at the eye tip radius $= \dfrac{\pi \times 1 \times 15000}{60}$

$$= 786 \text{ ft./sec.}$$

The peripheral speed at the eye root radius

$$= \frac{\pi \times 6{\cdot}5 \times 15000}{12{\cdot}60} = 425 \text{ ft. per sec.}$$

$$\alpha_1 \text{ at root} = \tan^{-1}\frac{469}{425} = 47^\circ\ 49'$$

$$\alpha_1 \text{ at tip} = \tan^{-1}\frac{469}{786} = 30^\circ\ 49'$$

The Diffuser.

The objects of the diffuser are :—

(1) To provide a smooth canalization of the flow of air from the impeller and to reduce to a minimum any turbulence which would otherwise be set up in the volute casing or ducts.

(2) To convert the kinetic energy to pressure energy. It must be stressed that it is much more difficult to obtain an efficient declaration of flow, than it is to obtain an efficient acceleration.

With the compressor running under its optimum conditions the vanes of the diffuser can be designed to pick up the air smoothly but there is a natural tendency for the air to break away from the surface in a diffusing system thus forming areas of turbulence. Consequently some of the kinetic energy is transferred into thermal energy instead of useful pressure energy. Undesirable temperature rises are also caused by the frictional effect of the high speed fluid flow through the diffuser channels. Experimental work has shown that the maximum permissible divergence of the diffuser channel is about 11°. Any increase in this figure results in higher losses.

We will now consider what happens to the air on leaving the impeller if the diffuser were not there, Fig. 4.

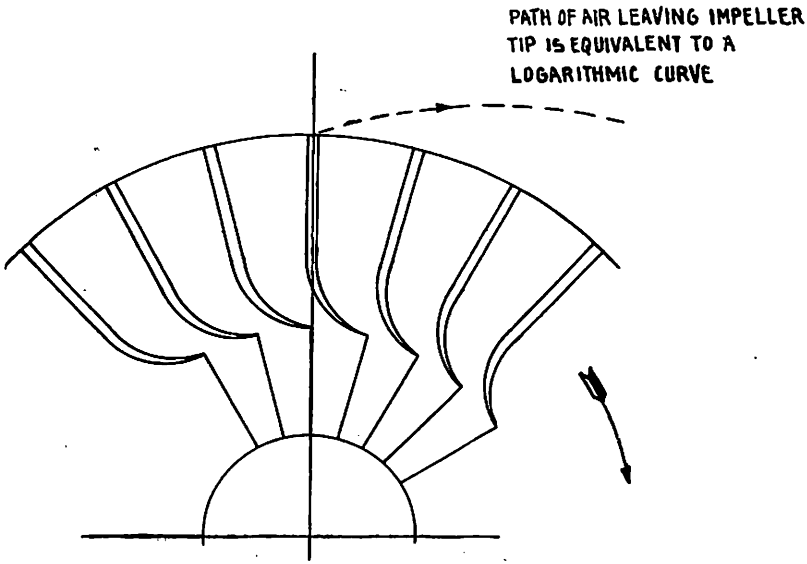

Fig. 4—Air Flow after Impeller Tip.

On leaving the impeller the air has an absolute velocity V_2, a tangential velocity Vw_2 and a relatively small velocity Vr_2. It follows that upon leaving the impeller its angular momentum remains constant, as no other forces act upon it which would alter its momentum. The angular momentum at any point is given by

$\dfrac{Q \times Vw_2 \times r}{g}$ and as the mass and momentum is constant the tangential component Vw_2 of the absolute velocity must be inversely proportional to the radial distance. Therefore the radial velocity Vr_2 will also decrease from the impeller tip to the diffuser vane, in accordance with the continuity equation. Since both components are inversely proportional to the radius, the absolute velocity is also proportional to the radius. Furthermore the angle which the direction of the absolute velocity V_2 makes with the tangential velocity Vw_2 at any point is constant. Thus we have the conditions for a logarithmic spiral which is the theoretical path of the air leaving the impeller.

Both Vr_2 and Vw_2 decrease after leaving the impeller tip then the resultant velocity V_2 will also decrease. This occurs in the vaneless space between the impeller tip and the diffuser and some diffusion will take place. For reasons which will be explained later the number of diffuser passages is less than the number of impeller blades.

We will now consider the design of a diffuser to be used with the impeller designed earlier. Certain dimensions have to be assumed and are as follows :—

Number of diffuser vanes,	13
Width of casing,	1·750 ins.
Radial width of vaneless space,	1·500 ins.
Mean radius of diffuser throat,	12·75 ins.

It will also be assumed that any losses are equally divided between the impeller and the diffuser. From the above data, radius of vane leading edges = 12 ins.

$Vwr \times r$ = constant. $\therefore$ whirl velocity of air at 12 ins. radius

$$= \frac{0{\cdot}9 \times 1371 \times 10{\cdot}5}{12} = 1079 \text{ ft. per sec.}$$

$$\text{Temperature equivalent} = \frac{1079^2}{2g \times J \times Cp} = \frac{1,164,241}{21,638{\cdot}4} = 53{\cdot}8^\circ$$

Now the radial velocity can be obtained from the continuity equation and as the density depends on the radial velocity Vr_2 a trial and error method must be used. The density changes only slightly for considerable changes in the radial velocity Vr_2, hence at least 5 figure logarithims should be used. Only the final trial will be given.

Assume Vr_2 to be 290 ft. per sec.

$$\text{Temperature equivalent} = \frac{290^2}{2g \times J \times Cp} = 3{\cdot}8^\circ\text{C.}$$

$\therefore$ Temperature equivalent of resultant velocity $= 53{\cdot}8 + 3{\cdot}8$
$= 57{\cdot}6°C.$

$T_2t - T_1t = 162{\cdot}6°C. \quad \therefore T_2t = 298{\cdot}2 + 162{\cdot}6 = 460{\cdot}8°K.$

But T_2t is the same for any radius after the impeller tip.

$\therefore$ T_2 at 12″ radius $= 460{\cdot}8 - 57{\cdot}6 = 403{\cdot}2°K.$

To find the static pressure P_2 and the density ϱ_2 we require to know the static temperature, on the assumption of isentropic compression up to the 12 in. radius.

$\therefore \quad T_2t - T_2t^1 = 39°C.$

As 50% of the losses occur before the diffuser T_2^1 at the 12 in., radius $= 403{\cdot}2 - 19{\cdot}5 = 383{\cdot}7°K.$

$$\frac{P_2}{P_1t} = \left(\frac{T_2^1}{T_1t}\right)^{\frac{y}{y-1}} \quad \therefore P_2 \text{ at 12 in, radius} = 16{\cdot}5 \left(\frac{383{\cdot}7}{298{\cdot}2}\right)^{3{\cdot}5}$$

$$= 16{\cdot}5 \times 2{\cdot}417 = 39{\cdot}882 \text{ lb. per sq. in.}$$

$$P_2 = \frac{144 \times 39{\cdot}882}{96 \times 403{\cdot}2} = 0{\cdot}1483 \text{ lb. per cu. ft.}$$

Area of cross section of flow at 12 in. radius $= \dfrac{2\pi \times 12 \times 1{\cdot}75}{144}$

$= 0{\cdot}916$ sq. ft.

Thus having Q, $\varrho 2$ and A we can check on the radial velocity $Vr2$ by means of the continuity equation :—

$$Vr2 = \frac{40}{0{\cdot}1483 \times 0{\cdot}916} = 294 \text{ ft. per sec.}$$

The angle of the diffuser vane leading edge is $\tan^{-1}\left(\dfrac{Vr_2}{Vw_2}\right)$

$$= \tan^{-1}\left(\frac{294}{1079}\right) = 15° - 15'$$

The next thing to consider is the throat width of the diffuser channels and this can be obtained by a similar process. The mean radius of the diffuser throat is 12·75 ins., and as the losses between a radius of 12 ins. and 12·75 ins. practically remain the same, we shall still consider 19·5°C. as this loss before the diffuser throat. Proceeding as before :—

Whirl velocity at 12·75 ins. rad. $= \dfrac{0{\cdot}9 \times 1371 \times 10{\cdot}5}{12{\cdot}75}$

$= 1016$ ft./sec.

Temperature equivalent $= \dfrac{1016^2}{2g \times J \times Cp} = 47{\cdot}7°C.$

Try a radial velocity of 275 ft. per sec.

Temperature equivalent $= \dfrac{275^2}{2g \times J \times Cp} = 3{\cdot}5^\circ C.$

Temperature equivalent of resultant velocity $= 47{\cdot}7 + 3{\cdot}5 = 51{\cdot}2^\circ C.$
T2 at 12·75 in. rad. $= 460{\cdot}8 - 51{\cdot}2 = 409{\cdot}6^\circ K.$
$T2^1$ at 12·75 in. rad. $= 409{\cdot}6 - 19{\cdot}5 = 390{\cdot}1^\circ K.$

$$P_2 = 16{\cdot}5 \left(\frac{390{\cdot}1}{298{\cdot}2}\right)^{3\cdot5} = 16{\cdot}5 \times 2{\cdot}560 = 42{\cdot}3 \text{ lb. per sq. in.}$$

$$C_2 = \frac{144 \times 42{\cdot}3}{96 \times 409{\cdot}6} = 0{\cdot}155 \text{ lb. per cu. ft.}$$

Neglecting the thickness of the vanes the area of flow in a radial direction $\doteq \dfrac{2\pi \times 12{\cdot}75 \times 1{\cdot}75}{144} = 0{\cdot}973$ sq. ft.

$$\therefore \; Vr_2 \text{ at } 12{\cdot}75 \text{ radius} = \frac{40}{0{\cdot}155 \times 0{\cdot}973} = 266 \text{ ft. per sec.}$$

$$\text{Angle of direction of flow} = \tan^{-1}\frac{266}{1016} = 14^\circ - 40 \text{ ft.}$$

The total throat area of the diffuser passages equals 0·973 sin. $14^\circ - 40' = 0{\cdot}246$ sq. ft.

The width of each throat must therefore be $\dfrac{0{\cdot}246 \times 144}{13 \times 1{\cdot}75}$
$= 1{\cdot}55$ ins.

In order to obtain the correct curvature of the vanes it is necessary to determine the logarithmic spiral from the data already obtained. It would be possible to obtain successive values for Vr and Vw_2, from which we would obtain a series of values for ϕ but this would be a lengthy process, hence we must resort to the logarithmic spiral.

The equation to a logarithmic spiral is $r = ae^{b\theta}$ where r = ray or radius length ; b is the coefficient of $\theta = \cot \alpha$ where $\alpha = 90^\circ - \phi$; θ = ray angle and a = initial radius. Obviously knowing ϕ at 12 in. radius this is a convenient point at which to commence the logarithmic spiral. Hence $\alpha = 90^\circ - \phi = 90^\circ - 15^\circ.$
$= 75^\circ$ and cot 75°.
$= 0{\cdot}26794.$

The equation now reads $r = 12e^{0\cdot26794\theta}$

$$\therefore \; r = 12e^{\frac{0\cdot26794a}{57\cdot3}} = 12e^{0\cdot00467a}$$

In log form $\log r = \log 12 + 0{\cdot}00467a \log e.$
$= 1{\cdot}0791812 + (0{\cdot}00467 \times 0{\cdot}4343a).$
$= 1{\cdot}0791812 + 0{\cdot}002028a.$

TABLE OF VALUES.

a	0°	5°	10°	15°	20°	25°	30°	35°	40°	45°
$0·002028a$	0	0·01014	0·02028	0·03042	0·04056	0·05070	0·06084	0·07098	0·08112	0·09126
$\log r$	1·0791812	1·08932	1·09946	1·10960	1·11974	1·12988	1·14002	1·15016	1·16028	1·17044
r	12	12·283	12·574	12·871	13·175	13·486	13·805	14·131	14·464	14·806

The above values can now be plotted on to the diffuser layout Fig. 5 where by using the appropriate radius to connect the plotted points we obtain the correct diffuser vane curvature. It will be seen from Fig. 5 that in order to obtain optimum conditions the direction of air flow after the throat should be in the direction as previously calculated, *i.e.*, 14° 37′, this being the angle of flow

at mean radius of throat area. However some amendment may be necessary in order to accommodate the diffuser into the general design of the engine but should be avoided as much as possible.

Compressibility Effects.

When the velocity of a compressible fluid, relative to the surface over which it is moving, reaches the speed of sound in the fluid, pressure losses occur.

When designing a centrifugal compressor the size of the unit is an important feature and the largest possible mass flow with the smallest compressor is the optimum aim. Air speeds are high, thus it is of great importance that the Mach numbers at certain points in the compressor do not exceed the value beyond which losses occur due to the formation of shock waves. Normally, the Mach numbers should not be allowed to exceed 0·8.

We will now consider the Mach numbers at various stages in the compressor, *i.e.*, (*a*) Impeller Intake ; (*b*) Impeller Passages ; (*c*) Diffuser.

(*a*) Impeller Intake.

Due to the curvature of the impeller blades the air at entry is deflected through a certain angle before it passes into the radial channels. There always exists a tendency for the air to break away from the trailing edge of the impeller eye, hence here is a point where the Mach number is extremely important and is shown in Fig. 6 (*a*).

Fig. 6 (*b*) illustrates the velocity triangle for the impeller eye and is shown in full line. It has been assumed that the inlet velocity Va_1 is constant all over the surface of the impeller, therefore the velocity of the entry air relative to the impeller designated by V_1 will reach a maximum at the eye tip of the impeller. The inlet Mach number will be given by :—

$$M = \frac{V_1}{\sqrt{g\gamma RT_1}} \qquad (14)$$

where T_1 is the static temperature at the inlet.

We will now consider the Mach number at inlet for the compressor being designed.

From previous calculations :—

Inlet velocity Va_1	$= 469$ ft. per sec.
Eye tip speed	$= 786$ ft. per sec.
Relative velocity at tip V_1	$= \sqrt{469^2 + 786^2} = 915$ ft. per sec.
Velocity of sound	$= \sqrt{32{\cdot}2 \times 1{\cdot}4 \times 96 \times 288}$
	$= 1116$ ft. per sec.

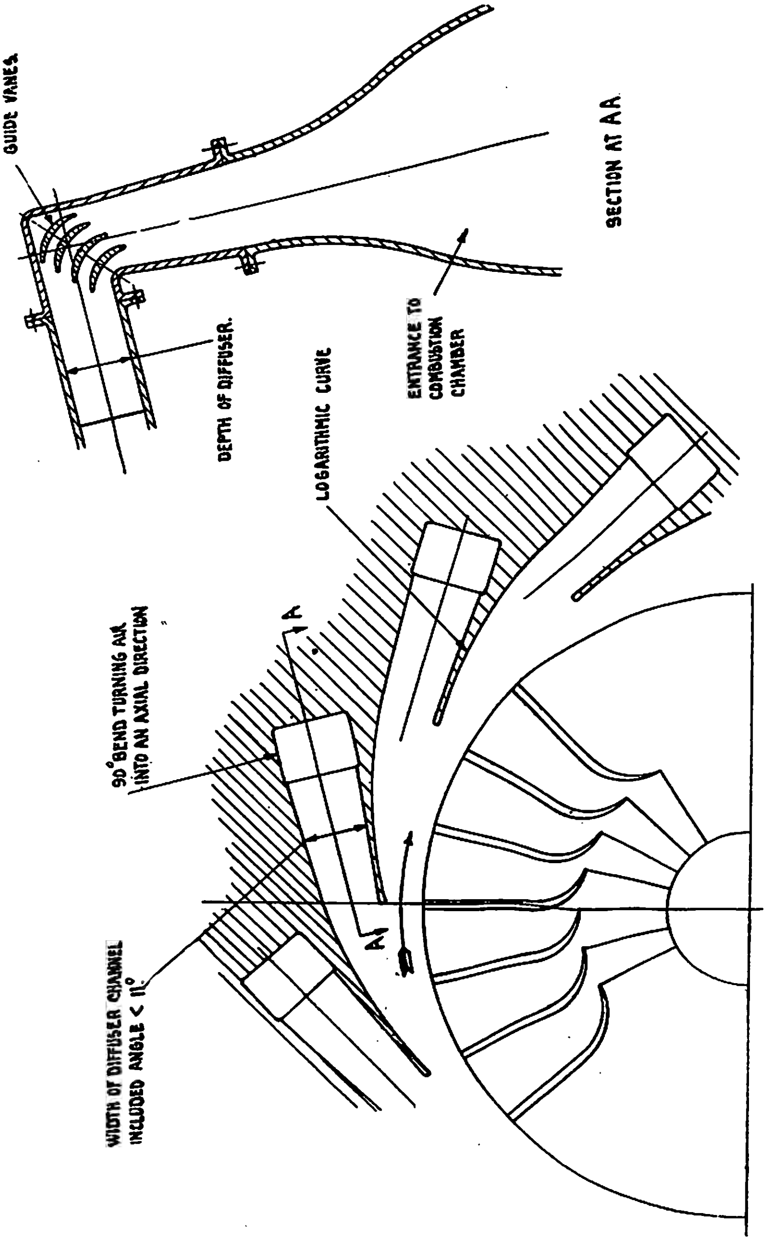

Fig. 5—Diffuser Layout.

$\therefore$ Maximum Mach number at inlet $= \dfrac{915}{1116} = 0{\cdot}82.$

This figure would be satisfactory under sea level conditions, but when operating at high altitudes with ambient temperature around 215°K. the Mach number would be much higher.

Thus we will consider the conditions experienced at an altitude of 40,000 ft. The effect of drop in atmospheric temperature will not be so great as may be imagined due to the ram effect at the intake when the aircraft has a forward speed. Assuming a normal speed of 375 m.p.h. the following data is obtained :—

$$\text{Temperature equivalent of forward speed} = \frac{550^2}{2g \times J \times Cp}$$
$$= 13{\cdot}98°\text{C}.$$

$$\therefore \text{ Inlet total head temperature} = 215°\text{K} + 13{\cdot}98°\text{C} = 228{\cdot}98°\text{K}.$$

$$\text{Temperature equivalent of axial inlet velocity} = 10{\cdot}2°\text{C}.$$

$$\therefore \text{ Inlet static temperature at 40,000 ft.} = 228{\cdot}98 - 10{\cdot}20.$$
$$= 218{\cdot}78°\text{K}.$$

$$\text{Mach number at inlet} = 0{\cdot}82\sqrt{\frac{288}{218{\cdot}78}} = 0{\cdot}940.$$

This then exceeds the permissible Mach number and it is, therefore, necessary to reduce the relative velocity V_1. It is possible to do this by means of introducing "prewhirl" at the intake. Curved vanes attached to the compressor casing deflect the incoming air and we obtain a velocity triangle as shown in Fig. 6 (*b*).

Unfortunately this method of reducing the relative inlet velocity V_1 reduces the work capacity of the compressor, by reason of the inlet air possessing a whirl velocity V_{w_1}. The rate of change of angular momentum per lb. of air per second now becomes :—

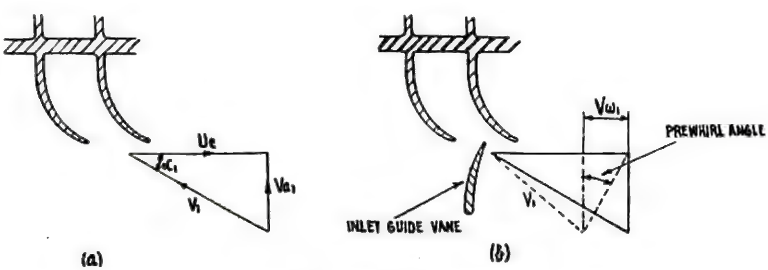

Fig. 6—Effect of Prewhirl.

$$\frac{V_{w2} . r_2 - V_{w1} r_1}{g} \text{ lb. ft.} \tag{15}$$

If it be assumed that V_{w_1} remains constant over the eye of the impeller, then the angular momentum must increase from root to tip. It follows that the amount of work done per lb. of air varies according to the radius at which the air enters the impeller eye. However, the Mach number is only high at the eye tip and it is preferable to vary the prewhirl from root to tip by means of twisting the inlet guide vanes so that the prewhirl value varies from zero to a maximum at the eye tip.

The angle of prewhirl is generally made 30° and a new value for the axial velocity must now be found by the usual trial and error process.

Only the final result will be shown.

$$\text{Try } Va_1 = 490 \text{ ft./sec.}$$

$$V_{a2} = \frac{490}{\cos 30°} = 565 \text{ ft./sec.}$$

Temperature equivalent of V_{a2} = 14·75°C.

$$T_1 = 298{\cdot}2 - 14{\cdot}75 = 283{\cdot}45\text{°K.}$$

$$P_1 = \frac{16{\cdot}5}{(1{\cdot}052)^{3{\cdot}5}} = 13{\cdot}818 \text{ lb. per sq. in.}$$

$$\rho 1 = \frac{13{\cdot}818 \times 144}{96 \times 283{\cdot}45} = 0{\cdot}0731 \text{ lb. per cu. ft.}$$

$$\text{Check on } V_{a1} = \frac{20}{0{\cdot}0734 \times \frac{\pi\,(12^2 - 6{\cdot}5^2)}{4 \times 144}} = 493 \text{ ft. per sec.}$$

Whirl velocity at inlet V_{w_1} = 490 tan 30° = 282 ft. per sec.

$$\text{Maximum relative velocity} = \sqrt{490^2 + (786 - 282)^2} = \sqrt{494{,}116}$$
$$= 703 \text{ ft. per sec.}$$

Maximum inlet Mac number when T_{1t} = 298·2°K.

$$= \frac{703}{\sqrt{32{\cdot}2 \times 1{\cdot}4 \times 96 \times 283{\cdot}45}} = 0{\cdot}634.$$

This is a satisfactory figure under altitude conditions.

Prewhirl has an effect on the pressure ratio and assuming that the prewhirl remains constant over the whole of the impeller eye :—

$$\text{Speed of eye at mean radius } U_e = \frac{786 + 425}{2} = 605{\cdot}5 \text{ ft. per sec.}$$

$$\text{Actual temperature rise} = \frac{p\,(\sigma\, U^2 - V_{w_1} \times Ue)}{g \times J \times Cp}$$

$$= \frac{1{\cdot}04\,(0{\cdot}9 \times 1371^2 - 282 \times 605{\cdot}5)}{32{\cdot}2 \times 1400 \times 0{\cdot}24} = 146{\cdot}2°\text{C.}$$

$$T_{2t_1} - T_{1t} = 0{\cdot}76 \times 146{\cdot}2 = 111{\cdot}11°\text{C.}$$

$$\therefore \frac{P_{2t}}{P_{1t}} = \left[1 + \frac{111{\cdot}11}{298{\cdot}2}\right]^{3{\cdot}5} = (1{\cdot}372)^{3{\cdot}5}$$

$$= 3{\cdot}02.$$

Mach Number in the Diffuser.

The maximum Mach number in the diffuser obviously occurs at the entry, that is, the impeller tip.

V_{w2} at impeller tip $= 0{\cdot}9 \times 1371 = 1233$ ft. per sec.

Try $V_{r2} = 390$ ft. per sec.

Resultant velocity $V_2 = \sqrt{1233^2 + 390^2} = 1293$ ft. per sec.

$$\text{Temperature equivalent} = \frac{1293^2}{2g \times J \times Cp} = 77{\cdot}28°\text{C.}$$

$T_{2t} = 460{\cdot}8°$K. $\therefore$ $T_2 = 460{\cdot}8 - 77{\cdot}28 = 383{\cdot}52°$K.

Again assuming a loss of 19·5°C. up to this point.

$$T_2^1 = 383{\cdot}5 - 19{\cdot}5 = 364°\text{K.}$$

$$\text{Now } \frac{P_2}{P_1 t} = \left(\frac{T_2 1}{T_1 t}\right)^{\frac{y}{y-1}} \quad \therefore P_2 = 16{\cdot}5\left(\frac{364}{298{\cdot}2}\right)^{3{\cdot}5}$$

$$= 33{\cdot}148 \text{ lb. per sq. in.}$$

$$\varrho 2 = \frac{33{\cdot}148 \times 144}{96 \times 383{\cdot}52} \doteq 0{\cdot}129 \text{ lb. per cu. ft.}$$

$$\text{Area of flow in radial direction at } 10{\cdot}5 \text{ rad.} = \frac{2\pi \times 10{\cdot}5 \times 1{\cdot}75}{144}$$

$$= 0{\cdot}801 \text{ sq. ft.}$$

$$\text{Checking value of } V_{r2} = \frac{40}{0{\cdot}129 \times 0{\cdot}801} = 387 \text{ ft. per sec.}$$

Thus the resultant velocity of 1293 ft. per sec. is satisfactory and therefore the Mach number at the impeller tip is :—

$$\frac{1293}{\sqrt{32{\cdot}2 \times 1{\cdot}4 \times 96 \times 383{\cdot}5}} = 1{\cdot}003.$$

We will now consider the Mach number at the diffuser leading tip edges. Using data already obtained the resultant velocity

$$= \sqrt{290^2 - 1079^2} = 1117 \text{ ft. per sec.}$$

The static temperature T2 at this radius was 403·2°K.

∴ the Mach number is

$$\frac{1117}{\sqrt{32{\cdot}2 \times 1{\cdot}4 \times 96 \times 403{\cdot}2}} = 0{\cdot}84.$$

From previous experimental work it has been found that Mach numbers greater than 1·00 can be used at the impeller tip but that high Mach numbers present at the leading edges of the diffuser are undesirable. Thus can now be easily seen the reason for the vaneless space. Circumferential pressure variations are set up when Mach numbers are high at the diffuser tip. These pressure variations cause vane vibrations which should they equal the natural frequency of the impeller then fatigue will occur. In order to reduce resonance the number of vanes in the impeller should not be a multiple of the vanes in the diffuser.

BIBLIOGRAPHY.

CONSTANT, H. ... "The Early History of the Axial Type of Gas Turbine Engine." (Proc.I.Mech.E., Vol. 153, W.E.P. No. 12, 1945).

COHEN & ROGERS "Gas Turbine Theory."

HOWELL, A. R. "Fluid Dynamics of Axial Compressors" and "Design of Axial Compressors." (Proc.I.Mech.E., Vol. 153, W.E.P. No. 12, 1945.)

TODD, K. W. ... "Practical Aspects of Cascade Wind Tunnel Research." (Proc.I.Mech.E., Vol. 157, W.E.P. No. 36, 1947).

A.E.S.D. Printed Pamphlets and Other Publications in Stock.

An up-to-date list of A.E.S.D. pamphlets in stock is obtainable on application to the Editor, *The Draughtsman*, Onslow Hall, Little Green, Richmond, Surrey.

A similar list is also published in *The Draughtsman* twice a year.

Readers are asked to consult this list before ordering pamphlets published in previous sessions.

List of A.E.S.D. Data Sheets

1. Safe Load on Machine-Cut Spur Gears.
2. Deflection of Shafts and Beams. } Connected.
3. Deflection of Shafts and Beams (Instruction Sheet). }
4. Steam Radiation Heating Chart.
5. Horse-Power of Leather Belts, etc.
6. Automobile Brakes (Axle Brakes). } Connected.
7. Automobile Brakes (Transmission Brakes). }
8. Capacities of Bucket Elevators.
9. Valley Angle Chart for Hoppers and Chutes.
10. Shafts up to $5\frac{1}{2}$ inch diameter, subjected to Twisting and Combined Bending and Twisting.
11. Shafts, $5\frac{3}{4}$ to 26 inch diameter, subjected to Twisting and Combined Bending and Twisting.
12. Ship Derrick Booms.
13. Spiral Springs (Diameter of Round or Square Wire).
14. Spiral Springs (Compression).
15. Automobile Clutches (Cone Clutches).
16. ,, ,, (Plate Clutches).
17. Coil Friction for Belts, etc.
18. Internal Expanding Brakes. Self-Balancing Brake Shoes (Force Diagram). } Connected
19. Internal Expanding Brakes. Angular Proportions for Self-Balancing. }
20. Referred Mean Pressure Cut-Off, etc.
21. Particulars for Balata Belt Drives.
22. $\frac{7}{8}''$ Square Duralumin Tubes as Struts.
23. 1″ ,, ,, ,, ,,
24. $\frac{3}{4}''$ Square Steel Tubes as Struts (30 ton yield).
25. $\frac{7}{8}''$,, ,, ,, (30 ton yield).
26. 1″ ,, ,, ,, (30 ton yield).
27. $\frac{3}{4}''$,, ,, ,, (40 ton yield).
28. $\frac{7}{8}''$,, ,, ,, (40 ton yield).
29. 1″ ,, ,, ,, (40 ton yield).
30. Moments of Inertia of Built-up Sections (Tables). } Connected.
31. Moments of Inertia of Built-up Sections (Instructions and Examples). }
34. Capacity and Speed Chart for Troughed Band Conveyors.
35. Screw Propeller Design (Sheet 1, Diameter Chart). } Connected.
36. ,, ,, ,, (Sheet 2, Pitch Chart). }
37. ,, ,, ,, (Sheet 3, Notes & Examples). }
38. Open Coil Conical Springs.
39. Close Coil Conical Springs.
40. Trajectory Described by Belt Conveyors (Revised, 1949).
41. Metric Equivalents.
42. Useful Conversion Factors.
43. Torsion of Non-Circular Shafts.
44. Railway Vehicles on Curves.
46. Coned Plate Development.
47. Solution of Triangles (Sheet 1, Right Angles).
48. Solution of Triangles (Sheet 2, Oblique Angles).
49. Relation between Length, Linear Movement and Angular Movement of Lever (Diagram and Notes).
50. ,, ,, ,, ,, ,, ,, (Chart).
51. Helix Angle and Efficiency of Screws and Worms.
52. Approximate Radius of Gyration of Various Sections.

53. Helical Spring Graphs (Round Wire). } Connected.
54. ,, ,, ,, (Round Wire).
55. ,, ,, ,, (Square Wire).
56. Relative Value of Welds to Rivets.
58. Graphs for Strength of Rectangular Flat Plates of Uniform Thickness.
59. ,, Deflection ,, ,, ,, ,, ,,
61. Deflection of Leaf Spring.
62. Strength of Leaf Spring.
63. Chart Showing Relationship of Various Hardness Tests.
64. Shaft Horse-Power and Proportions of Worm Gear.
65. Ring with Uniform Internal Load (Tangential Strain) } Connected.
66. ,, ,, ,, ,, (Tangential Stress)
67. Hub Pressed on to Steel Shaft. (Maximum Tangential Stress at Bore of Hub).
68. Hub Pressed on to Steel Shaft. (Radial Gripping Pressure between Hub and Shaft).
69. Rotating Disc (Steel) Tangential Strain. } Connected.
70. ,, ,, ,, Stress.
71. Ring with Uniform External Load, Tangential Strain. } Connected.
72. ,, ,, ,, ,, ,, Stress.
73. Viscosity Temperature Chart for Converting Commercial to Absolute Viscosities. } Connected.
74. Journal Friction on Bearings.
75. Ring Oil Bearings.
76. Shearing and Bearing Values for High Tensile Structural Steel Shop Rivets, in accordance with B.S.S. No. 548/1934.
78. Velocity of Flow in Pipes for a Given Delivery. } Connected.
79. Delivery of Water in Pipes for a Given Head.
80. (See No. 105).
81. Involute Toothed Gearing Chart.
83. Variation of Suction Lift and Temperature for Centrifugal Pumps.
89. Curve Relating Natural Frequency and Deflection. } Connected
90. Vibration Transmissibility Curved or Elastic Suspension.
91. Instructions and Examples in the Use of Data Sheets, Nos. 89 and 90.
92. Pressure on Sides of Bunker.
93-4-5-6-7. Rolled Steel Sections.
98-9-100. Boiler Safety Valves.
102. Pressure Required for Blanking and Piercing.
103. Punch and Die Clearances for Blanking and Piercing.
104. Nomograph for Valley Angles of Hoppers and Chutes.
105. Permissible Working Stresses in Mild Steel Struts with B.S. 449, 1948.
106. Compound Cylinder (Similar Material) Radial Pressure of Common Diameter (D1).

(Data Sheets are 3d to Members, 6d to others, post free).

Orders for Pamphlets and Data Sheets to be sent to the Editor, *The Draughtsman*, cheques and orders being crossed "A.E.S.D."